TAMOXIFEN MEDIATED METABOLIC STRESS: MOLECULAR MECHANISM AND THERAPEUTIC OPPERTUNITIES

Natalie A. Daurio

A DISSERTATION

in

Pharmacology

Presented to the Faculties of the University of Pennsylvania

in

Partial Fulfillment of the Requirements for the

Degree of Doctor of Philosophy

2016

Supervisor of Dissertation

_____

Constantinos Koumenis, Ph.D., Professor of Radiation Oncology

Graduate Group Chairperson

_____

Julie Blendy, Ph.D., Professor of Pharmacology

Dissertation Committee

Jim Delikatny, Ph.D., Research Associate Professor of Radiology

Ian Blair, Ph.D., A.N. Richards Professor of Pharmacology

Andy Minn, M.D., Ph.D., Associate Professor of Radiation Oncology

Xiaolu Yang, Ph.D., Professor of Cancer Biology

TAMOXIFEN MEDIATED METABOLIC STRESS: MOLECULAR MECHANISM AND

THERAPEUTIC OPPERTUNITIES

ACKNOWLEDGMENT

First, I would like to acknowledge and thank my advisor, Dr. Costas Koumenis, for your support and mentorship throughout the past 5 years. During my time in the lab I not only learned the skills necessary to be an independent and diligent scientist but have also grown as a person, gaining the resiliency and confidence in myself necessary for a future career as a successful scientist. I truly appreciate your willingness to allow me to pursue a project in an area that was fairly new to the lab in cancer metabolism and allowing me to incorporate my experience and passion for chemistry into the project. I also really appreciate the many opportunities provided for me to present my work both in formal presentations at Penn as well as at international conferences. These experiences have shaped me into a skilled scientific communicator, a quality that will be invaluable in my future scientific career.

Next, I would like to thank my thesis committee, Jim Delikatny, Ian Blair, Xiaolu Yang and Andy Minn for their thoughtful suggestions, insight, advice, and support during the course of my dissertation research. You helped to strengthen my work and encouraged my growth as a scientist throughout my training.

I would also like to acknowledge all the past and present members of the Koumenis lab: Steve Tuttle, Souvik Dey, John Verginadis, Feven Tamiere, Lauren Brady, Alexandra Monroy, Cindy Bi, Stacey Lehman, Carly Sayers, Lori Hart, Vladimir Popov, Yi Chen, David Guttman, Julianne Davis, and Ethan Song. Thank you for your technical assistance, advice and feedback, support, and friendship throughout my time in the lab. You made coming to lab enjoyable daily and I will miss working with all of you.

I would also like to extent an extra special thanks to Steve Tuttle. This project would not have been possible without your biochemistry and metabolism expertise as well as your technical training and advice and support. Thank you for all your help with

the animal experiments, oxygen consumption measurements and glycolytic inhibition experiments. I would also like to acknowledge Julianne Davis and Ethan Song, undergraduate students who worked in the lab on this project. Thank you for all your effort and patience. Acknowledgement and thanks must be extended to Ian Blair, Andrew Worth, and Nate Snyder for the LC-MS/MS data and metabolic pathway expertise. I would also like to thank George Cerniglia and Amit Maity for their assistance in the oxygen consumption experiments and mTOR pathway analysis. I also must thank Steve Kridel at Wake Forest University for his help with the ^{14}C-acetate lipid experiments.

I would also like to thank Jenine Iannaccone, Christie Foti, Chiharu Sako, and Donna Seravello for all their help with scheduling, travel, purchasing and funding. Having their support and assistance with all administrative tasks made it much easier to focus on science.

Next, I would like to thank my friends in RadOnc, especially Michele, Lauren, Alan, and Richard, and BGS especially Rosemary Challis, and all the other PGG students. Thank you for all your friendship, support and the many good memories at Penn.

Finally, I would like to thank my parents and sister. Thank you for your never ending support and love. You have always believed in me and encouraged all my academic endeavors. I could not have done this without you!

ABSTRACT

TAMOXIFEN MEDIATED METABOLIC STRESS: MOLECULAR MECHANISM AND THERAPEUTIC OPPERTUNITIES

Natalie A. Daurio

Constantinos Koumenis

Tamoxifen is the most widely used adjuvant chemotherapeutic for the treatment of estrogen receptor (ER) positive breast cancer, yet a large body of clinical and preclinical data indicates that tamoxifen can modulate multiple cellular processes independently of ER status. Here, we describe the ER-independent effects of tamoxifen on tumor metabolism. Using combined pharmacological and genetic knockout approaches, we demonstrate that tamoxifen inhibits oxygen consumption via inhibition of mitochondrial complex I, resulting in an increase in the AMP/ATP ratio and activation of the AMPK signaling pathway *in vitro* and *in vivo*. We also show that tamoxifen-induced cytotoxicity is modulated by isoform-specific effects of AMPK signaling, in which AMPKα1 promotes cell death through inhibition of the mTOR pathway and translation. Tamoxifen treatment also reprograms cellular metabolism by promoting glycolysis, and altering fatty acid metabolism, leading to the depletion of intracellular lipid stores. By using agents which target concurrently distinct adaptive responses to tamoxifen-mediated metabolic reprogramming, we demonstrate increased cytotoxicity. Tamoxifen synergizes with glycolytic inhibitors to kill breast cancer cells and can preferentially kill oxidative phosphorylation-dependent populations. Our results demonstrate novel metabolic perturbations by tamoxifen in tumor cells which can be exploited to expand the therapeutic potential of tamoxifen treatment beyond ER+ breast cancer.

TABLE OF CONTENTS

LIST OF TABLES

LIST OF FIGURES

CHAPTER 1: GENERAL INTRODUCTION

Breast cancer (BC) is responsible for 1.1 million cancer diagnoses annually world wide and 410,000 deaths[1]. It is second leading cause of cancer related deaths in women in the United States. Breast cancer deaths are not the result of the primary tumor but of recurrent and metastatic disease. Approximately 10-15% of patients will develop metastatic disease in the first 3 years following diagnosis however, the development of metastatic lesions after 10 years or more following treatment of the primary tumor is not unusual[2]. Therefore breast cancer patients remain at risk for metastatic disease for their entire life.

Breast cancer is a highly heterogeneous disease with distinct histopathological and molecular features that impact disease treatment and prognosis. As a result, a classification system with distinct BC subtypes is used to guide clinical decision making in combination with traditional variables such as tumor size, invasiveness, and node involvement. While scientific reports propose multiple different classification schemes, BC can be divided into three categories: luminal BC, which usually express estrogen receptor (ER) and/or progesterone receptor (PR), human epidermal growth factor receptor 2 (HER2) overexpressing BC, and basal BC. Basal BC is also known as triple negative BC referencing the lack of significant ER, PR, or HER2 expression and is the most heterogeneous subtype. Triple negative BC is also the most aggressive disease and is without any standard targeted therapy options.[3]

Tamoxifen is the most widely used non-steroidal selective estrogen receptor modulator (SERM) for adjuvant therapy of estrogen receptor-positive (ER^+) breast cancer (BC). SERMs are unique in that they exert ER agonist or antagonist properties in a tissue specific manner. Originally designed as a contraceptive, then used as a fertility agent, tamoxifen has been in the clinic since 1966. Patients on standard treatment receive tamoxifen at 20 mg/day for 5 years with initiation during, or shortly after, surgical

removal of the primary tumor and treatment with ionizing radiation or cytotoxic chemotherapy. Tamoxifen therapy has reduced disease recurrence by half and overall mortality by one-third in ER^+ BC patients[4]. As an anti-cancer agent tamoxifen has a relatively safe toxicity profile with the most common side effects including hot flashes and irregular menses. Due to its SERM effects, Tamoxifen treatment is also linked to an increased risk for endometrial cancer and rare thromboembolic events. However other positive effects have been reported such as an increase in bone mineral density in post-menopausal women as well as a decrease in total cholesterol and LDL levels that may contribute to a decrease in cardiovascular events that are seen in treated populations[4]. The development of tamoxifen resistance remains a significant clinical problem. Approximately one-third of women treated with tamoxifen will develop recurrent disease. Tamoxifen resistant tumors can be treated with second-generation anti-estrogenic therapies but total endocrine resistance often emerges. Only about 15% of these tamoxifen-resistant cases will lose ER expression. Additional mechanisms for the emergence of resistance are not well understood but have been reported to include changes in receptor post-translational modifications, altered downstream signal transduction, cross-talk with other growth receptors, and changes in expression of co-activators and other transcription factors[5].

The anti-tumor effects of tamoxifen are attributed primarily to its antiproliferative activity via competitive inhibition of the ER in breast tissue[6]. Several studies have previously described non-ER dependent effects of tamoxifen such as the inhibition of protein kinase C (PKC)[7–9] and the sensitization of ER-negative tumors to chemotherapeutic agents[10–12]. Furthermore, during the past two decades, over 25 clinical trials have been published reporting the effects of “high dose” tamoxifen (i.e. doses above those needed to inhibit tumor cell ER activity) ranging from 80 to 720

mg/day[12] to treat non-breast cancers including glioma[13–16], melanoma[17,18] and others[19,20], as a single agent or in combination with chemotherapeutics. While these Phase I and II trials showed variable clinical benefit, they clearly demonstrated the safety of high dose tamoxifen in diverse patient populations. Pharmacodynamic analyses indicated that tamoxifen could reach plasma concentrations as high as 8 μM[19] and additional preclinical studies indicated that tamoxifen accumulates in tumor tissue at 60-70 times the plasma concentration[21]. Therefore, further studies on "high dose" tamoxifen are clinically relevant and may result in expanded indications for this affordable and well-tolerated chemotherapeutic.

The chemical properties of tamoxifen as a lipophilic weak base contribute to its high partition into lipid bilayers and tamoxifen has been previously described to have inhibitory effects on mitochondrial respiratory rate[22] and membrane potential[23]. Agents targeting metabolic processes are of particular interest for cancer therapies due to the unique metabolic phenotype exhibited by tumors. As rapidly proliferating masses of cells, tumors require large pools of macromolecules to generate the proteins, lipids, and nucleotide content necessary to divide as well as sufficient quantities of ATP and reducing equivalents to power these processes[24]. In 1926, Otto Warburg first described the preference of cancer cells for converting glucose to lactate via glycolysis, even under sufficient oxygenation, an effect that is known as The Warburg Effect, or "aerobic glycolysis"[25]. He hypothesized that this occurs due to defects in cancer mitochondria, leaving cancer cells dependent on glycolysis for ATP production. However, more recent research has shown that cancer mitochondria are quite functional and has suggested that this elevation in glycolysis results from the need for precursor molecules from glycolytic intermediates for synthesis of fatty acids, nucleotides and amino acids. Tricarboxylic acid (TCA) cycle intermediates can also be used as carbon sources for

biosynthetic pathways[26]. Elevated glutamine uptake seen in cancer also contributes carbons to these synthetic pathways necessary for rapid cell division[24].

Metabolic processes are highly regulated and to achieve the phenotype necessary for rapid proliferation tumor promotion by certain oncogenes alter the metabolic characteristics of cells as a requirement for transformation [27]. Oncogenes including myc, nuclear factor-κB (NF- κB), AKT, various tyrosine kinase growth factor receptors, Ras, phosphatidylinositol 3-kinases (PI3Ks) and mammalian target of rapamycin (mTOR) pathways, and hypoxia- induced factors (HIFs) all enhance transcription of factors that promote glycolysis and glutaminolysis. Myc activation also promotes an increased rate of protein synthesis. Additionally, changes in metabolic enzymes themselves also play a role in tumor promotion including mutations in isocitrate dehydrogenase 1 (IDH1), succinate dehydrogenase and fumarase[28]. Tumor suppressors such as p53 and PTEN also play a role in metabolic transformation. Mutations or loss of expression of these genes have been shown to promote the aerobic glycolysis phenotype[29].

The cancer metabolic phenotype is essential for the survival and growth of tumors, making these pathways appealing therapeutic targets. Antimetabolites were the first successful cancer therapies to halt tumor growth by interfering with the ability to synthesize required molecules. DNA replication was targeted with small molecules analogs of essential purine and pyrimidine metabolites including methotrexate, 5-fluoruracil, and gemcitabine[30]. Many therapeutic strategies have also been employed to target the dependence of cancer on glycolysis, including use of glucose analogs such as 2-deoxy-glucose (2-DG) and inhibition of glycolysis enzymes including hexokinase II (HK2), glyceraldehyde 3-phosphate dehydrogenase (GAPDH), and phosphofructokinase (PFK), as well as blocking the export of lactate, and use of carbohydrate restricted

diets[31]. Amino acid metabolism has been another focus of drug development efforts. Inhibition of glutamine uptake and metabolism has shown some preclinical promise and L-aspariginase has been used clinically as a successful treatment for leukemia. Significant effort has also been directed towards developing inhibitors of fatty acid synthesis enzymes including fatty acid synthase (FASN), ATP citrate lyase (ACLY), and acetyl-CoA carboxylase (ACC). The success of these therapies targeting metabolic pathways have been limited by normal tissue toxicity as well as by metabolic plasticity or metabolic pathway redundancy that allows cells to overcome a blockade by upregulation of compensatory pathways[27,32]. As a result, combination therapies targeting multiple arms of metabolic pathways or the combination of a metabolic therapy with a cytotoxic chemotherapeutic are likely to be more successful.

Targeting of oncogenes that promote the cancer metabolic phenotype is another area of drug discovery research that has gained momentum in recent years. The term “oncogene addiction” describes tumor dependence on specific oncogene signaling pathways for continued tumor maintenance and progression. In these cases, deprivation of oncogene signaling results in tumor regression, therefore, these genes are the focus of targeted therapeutic development. Many of these oncogenes contribute to the cancer metabolic phenotype and pathway blockade often results in significant metabolic alterations. Targeting of mutant BRAF in melanoma and KRAS in pancreatic cancer, results in a reversal of the Warburg effect. Inhibition of PI3K, AKT, and mTOR has long been of interest due to their role in cell proliferation. Blockade of these pathways have been reported to result in both inhibition of glycolysis as well as oxidative phosphorylation[33,34]. The combination of these oncogene-targeted therapies with inhibitors of compensatory metabolic pathways may also increase efficacy and prevent resistance.

While upregulation of glycolytic and biosynthetic metabolic pathways plays an essential role in tumor progression, the function of mitochondrial respiration in cancer biology should not be discounted. Oxidative phosphorylation has been reported to provide 25-60% of the ATP pools for cancer cells and substrate availability has been shown to regulate oxidative capacity. Therefore, at times of glucose deprivation, mitochondria respiration may increase to maintain cellular function and the use of glutamine as a carbon source requires mitochondrial oxidative capacity[35]. Electron transport also functions to regenerate nicotinamide adenine dinucleotide (NAD+) and flavin adenine dinucleotide (FAD)[35]. Moreover, TCA cycle intermediates are required for synthesis of amino acids and nucleotides from both glucose and glutamine. Oxidative phosphorylation (OXPHOS) regeneration of reducing equivalents is necessary for continued TCA cycle activity[36]. Cancer heterogeneity also highlights the importance of mitochondrial metabolism in cancer. Cancer stem cells and tumor initiating cells have been showed to have higher levels of OXPHOS[37,38]. Respiration has also been shown to support the extravasation and intravasation processes required for metastasis[39]. Moreover, aggressive and drug resistant populations also characteristically have increased levels of OXPHOS[38,40]. Dormant cancer cells also may also depend on respiration to survive nutrient depleted conditions, allowing for cancer recurrence[37,41].

Since mitochondrial oxidative phosphorylation plays a significant role in cancer promotion, pharmacological inhibition of respiration may be an important drug target for the advancement of therapeutic options. Evidence from current literature supports the efficacy of this strategy. Metformin targeting of complex I of the electron transport chain has been shown to reduce tumorigenesis[42]. Resistance to targeted therapies in BRAF and KRAS driven tumors limits the therapeutic options in cancers such as melanoma and pancreatic cancer. The drug resistant populations are thus dependent on elevated

OXPHOS and drugs that target mitochondrial metabolism, such as biguanides, have potential utility in targeting such resistant populations by synthetic-lethality approaches [38,40,43–45]. Moreover, tumor hypoxia is a significant obstacle to the clinical success of ionizing radiation and other DNA damaging agents. Inhibition of mitochondrial respiration has been validated as a strategy to reduce tumor hypoxia and sensitize tumors to these therapies[46].

One of the consequences of OXPHOS inhibition, especially in metabolically active cancer cells, is the activation of the AMP-activated protein kinase (AMPK), the major regulator of cellular energy homeostasis. AMPK is activated when the AMP:ATP ratio increases, signaling a loss in cellular energy charge. Once activated, AMPK restores cellular energy levels by promoting catabolic and inhibiting anabolic processes[47]. AMPK is universally expressed across all eukaryotes as a heterotrimeric protein composed of an alpha catalytic subunit, and beta and gamma regulatory subunits. The gamma subunit contains four surface adenyl binding sites containing tandem repeats known as CBS repeats. Mammalian AMPK has a constitutively bound AMP at site 4 while site 2 remains unoccupied. AMP and ATP compete for binding at sites 1 and 3[48–50]. Interestingly, expression of adenylate kinase maintains the reaction $2ADP \leftrightarrow AMP+ATP$ at equilibrium. Therefore any loss in cellular energy levels will result in an increase in both AMP and ADP. However, since intracellular AMP pools are much smaller than ADP pools, their relative increase will be more significant making it logical that AMPK is most sensitive to the AMP/ATP ratio. When AMP binds these sites, a conformational change is induced that prevents the dephosphorylation of the catalytic alpha subunit of AMPK by phosphatases and enhances phosphorylation by upstream kinases. More specifically, binding at site 1 results in allosteric activation of AMPK and binding at site 3 promotes phosphorylation. The alpha subunit is phosphorylated on

Thr172 in the activation loop increasing kinase activity of the Ser/Thr kinase domain at the amino terminus[50].

The best described AMPK-kinase is liver kinase B1 (LKB1). LKB1 is a known tumor suppressor and is mutated in the inheritable Peutz-Jeghers syndrome characterized by benign intestinal polyps and mucocutaneous pigmentation with an increased risk for developing tumors of multiple lineages. LKB1 functions in a complex with ste20-related adaptor (STRAD) and mouse protein 25 (MO25). Activation of AMPK by metabolic stress has been shown to be diminished in LKB1-null cells[51]. AMPK can also be activated by calcium-calmodulin kinase kinase 2 (CaMKK2), linking changes in intracellular [Ca^{2+}] to activation of AMPK. Many other kinases have been reported to phosphorylate AMPK including transforming growth factor β-activated kinase (TAK1) and sestrins[47].

Once activated, AMPK signals downstream to restore cellular energy charge. AMPK promotes glycolysis through increased glucose transporter (GLUT) 1 and 4 expression increasing glucose uptake as well as activation of 6-phosphofructo-2-kinase/fructose-2,6-biphosphatase (PFKFB). AMPK also reduces protein synthesis through phosphorylation of tuberous sclerosis complex 2 (TSC2) and raptor resulting in inhibition of the mTOR pathway. Activation of AMPK promotes autophagy through direct phosphorylation of unc-51 like autophagy activating kinase 1 (ULK1) as well as through inhibition of mTOR. Moreover, AMPK inhibits fatty acid synthesis by inhibiting ACC, the enzyme responsible for converting acetyl-coA to malonyl-CoA the initial and rate limiting step of fatty acid synthesis. In addition, AMPK promotes beta oxidation of fatty acids by promoting the transcription of lipogenic enzymes via sterol regulatory element-binding transcription factor 1 (SREBP1) [48,50].

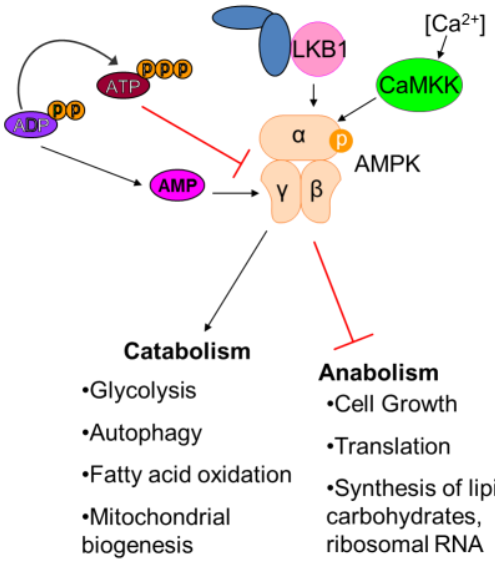

Figure I-1: AMP-Activated Protein Kinase (AMPK) Pathway: AMPK is a heterotrimeric protein that is activated by an increase in the AMP/ATP Ratio. Binding of AMP at the γ subunit promotes phosphorylation of the α catalytic subunit by upstream kinases including LKB1 and CamKK2. Once activated AMPK feeds downstream to turn off ATP consuming processes and activate ATP generating processes.

The role of AMPK in cancer is quite complex as it has been reported to function contextually as both a tumor suppressor or tumor promoter [49]. AMPK can function as a tumor promoter by helping cancer cells to survive and adapt to metabolic stress that is characteristic of tumor microenvironments and oncogene activation. AMPK activation can allow cells to switch between fuel sources including glucose, glutamine and fatty acids, in order to tolerate nutrient deprivation and may activate a cell cycle arrest to allow tumor cells to survive particularly lean conditions. AMPK also plays a pro-survival role through activation of autophagy[49].The role of AMPK as a mediator of the tumor suppressor properties of LKB1 has also been the focus of much research. Whole body knock out of AMPKα1 resulted in an increase in c-myc lymphoma development[52] and expression of a dominant negative AMPK promoted prostate cancer cell proliferation[53]. Moreover, patients on metformin, an AMPK activator used in diabetes treatment, have

been reported to have a lower incidence of cancers than metformin-naive diabetics[48]. Some of the tumor suppressor effects of AMPK have been attributed to its role in suppression of macromolecular synthesis pathways and its suppression of the Warburg effect. While acute AMPK activation promotes glycolysis, long term activation shifts cells towards a more oxidative phenotype by promoting mitochondrial biogenesis and transcription of oxidative enzymes. Moreover, inhibition of the mTOR pathway decreases translation of Hif-1α, a transcription factor that drives the Warburg effect[51,52]. Additional tumor suppressor functions of AMPK include the activation of cell cycle arrest through the stabilization of p53, p21 and p27[51]. Due to the decreased cancer incidence in metformin treated patients, considerable research has been directed towards developing metformin and other AMPK activators as cancer therapeutics.

Hypothesis:

Based on published studies mentioned above and our preliminary results with tamoxifen and OXPHOS, we formulated the central hypothesis that tamoxifen inhibits oxygen consumption through an ER-independent direct effect on the mitochondria that results in significant alterations in metabolism and cell signaling that can be exploited for therapeutic benefit. To test this hypothesis, we first investigated the mechanism by which tamoxifen inhibits oxygen consumption. This work demonstrated that tamoxifen inhibits oxygen consumption by acting directly on the mitochondria, upstream of complex II and independently of ER signaling. We then characterized the consequences of tamoxifen inhibition of OXPHOS on cell signaling and metabolism. We have shown that tamoxifen treatment results in a rapid and robust activation of the AMPK pathway *in vitro* and *in vivo*, and downstream effects are mediated in an isoform specific manner. Tamoxifen treatment also results in an increase in glycolysis and alterations in fatty acid metabolism. We then determined if the metabolic effects of tamoxifen can be used for therapeutic benefit. This work demonstrates that combination of tamoxifen and glycolytic inhibitors synergize to cause increased cytotoxicity and that tamoxifen inhibition of OXPHOS can be used to target OXPHOS addicted cancer populations. Overall, this work describes a novel mechanism of action for an extensively used drug and identifies new therapeutic opportunities.

CHAPTER 2: TAMOXIFEN INHIBITS MITOCHONDRIAL COMPLEX I AND ACTIVATES THE AMPK PATHWAY.

Sections of this chapter contribute to the published manuscript:

Natalie A. Daurio, Stephen W. Tuttle, Andrew J. Worth, Ethan Y. Song, Julianne M. Davis, Nathaniel W. Snyder, Ian A. Blair, and Constantinos Koumenis. **AMPK activation and metabolic reprogramming by tamoxifen through estrogen receptor-independent mechanisms suggests new uses for this therapeutic modality in cancer treatment.** *Cancer Res* OnlineFirst March 28, 2016.

Introduction:

The anti-tumor effects of tamoxifen in BC are attributed primarily to its antiproliferative activity via competitive inhibition of the ER in breast tissue [6]. Several studies have previously described non-ER dependent effects of tamoxifen such as the inhibition of Protein Kinase C (PKC)[9] and the sensitization of ER-negative tumors to chemotherapeutic agents[10]. Furthermore, during the past two decades, over 25 clinical trials have been published reporting the effects of "high dose" tamoxifen (i.e. doses above those needed to inhibit ER activity) ranging from 80 to 720 mg/day [12] to treat non-breast cancers including glioma[16], melanoma[17] and others[19,20], as a single agent or in combination with chemotherapeutics. While these Phase I and II trials showed variable clinical benefit, they clearly demonstrated the safety of high dose tamoxifen in diverse patient populations. Pharmacodynamic analyses indicated that tamoxifen could reach plasma concentrations as high as 8 μM[19] and additional preclinical studies indicated that tamoxifen accumulates in tumor tissue at 60-70 times the plasma concentration[21]. Therefore, further studies on "high dose" tamoxifen are clinically relevant and may result in expanded indications for this affordable and well-tolerated chemotherapeutic.

The chemical properties of tamoxifen as a lipophilic weak base contribute to its high partition into lipid bilayers and tamoxifen has been previously described to have inhibitory effects on mitochondrial respiratory rate[22] and membrane potential[23]. Cells in which oxidative phosphorylation (OXPHOS) is inhibited by pharmacologically targeting members of the mitochondrial respiratory chain, or due to lack of oxygen (hypoxia), exhibit a compensatory increase in glycolysis. For example, metformin, a diabetes drug showing promise as a cancer therapeutic, was recently demonstrated to inhibit Mitochondrial complex I and to upregulate glycolysis [42].

One of the consequences of OXPHOS inhibition, especially in metabolically active cancer cells, is the activation of the AMP-activated protein kinase (AMPK), the major regulator of cellular energy homeostasis. AMPK is activated when the AMP:ATP ratio increases, signaling a loss in cellular energy charge. AMP binds to the gamma subunit of AMPK inducing a conformational change that prevents the dephosphorylation of the catalytic alpha subunit of AMPK by phosphatases. This enhances phosphorylation of AMPK by upstream kinases including LKB1 and CaMKK2. Once activated, AMPK restores cellular energy levels by promoting catabolic and inhibiting anabolic processes[47]. The role of AMPK in cancer is quite complex as it has been reported to function contextually as both a tumor suppressor or promoter[49].

Based on these studies, we investigated whether tamoxifen had an impact on cellular metabolism and metabolic signaling. Here we report the ability of tamoxifen to inhibit oxygen consumption, through a direct effect on mitochondria, upstream of complex II. We also observe rapid (<10 min) and acute activation of AMPK *in vitro* and *in vivo* in an ER-independent manner. Moreover, we demonstrate that activation of the AMPK pathway by tamoxifen promotes cell death in triple-negative breast cancer cells in an AMPK-isoform specific manner.

Results:

While tamoxifen has been reported to affect mitochondrial electron transport and membrane potential, its effects on oxygen consumption have not been adequately described. A Clark electrode was used to measure oxygen consumption of cells. Tamoxifen, at low μM doses, inhibited oxygen consumption in a dose dependent manner in both ER^+ MCF7 cells and triple-negative MDA-MB-231 cells (Figure II-1A). Tamoxifen

also inhibited oxygen consumption in a panel of 6 non-breast cancer cell lines including prostate, glioma, lung and cervical cancer cell lines (Figure II-1B). The active metabolite of tamoxifen, 4-hydroxy-tamoxifen (4OH-Tam) also inhibited oxygen consumption while the ER antagonist fulvestrant, which inhibits ER activity by blocking ER dimerization and promoting degradation of the ER [54], did not have a significant effect on oxygen consumption. Interestingly, supra-physiologic doses of estradiol, the endogenous ligand of the ER, also inhibited BC cell oxygen consumption (Figure II-1C). This suggests that inhibition of ER signaling is not responsible for the rapid inhibition of oxygen consumption in response to tamoxifen treatment. To further rule out involvement of ER signaling in tamoxifen-mediated inhibition of oxygen consumption, we used both pharmacological and genetic means to knock down ER expression. Treatment of MCF7 cells with fulvestrant reduced ER expression (Figure II-1D insert). Subsequent treatment with tamoxifen recapitulated the dose dependent effects on oxygen consumption seen with the control treated MCF7 cells (Figure II-1D). We then used the CRISPR-Cas9 system to knock out ERα from LCC1 cells, a variant of the MCF7 line which expresses functional ER but is not dependent on its signaling for proliferation (Figure II-1E)[55]. The ability of tamoxifen to inhibit oxygen consumption in the LCC1-crspER cells was no different from the parental LCC1 cells (Figure II-1F) further supporting the notion that tamoxifen inhibits oxygen consumption independently of ER signaling.

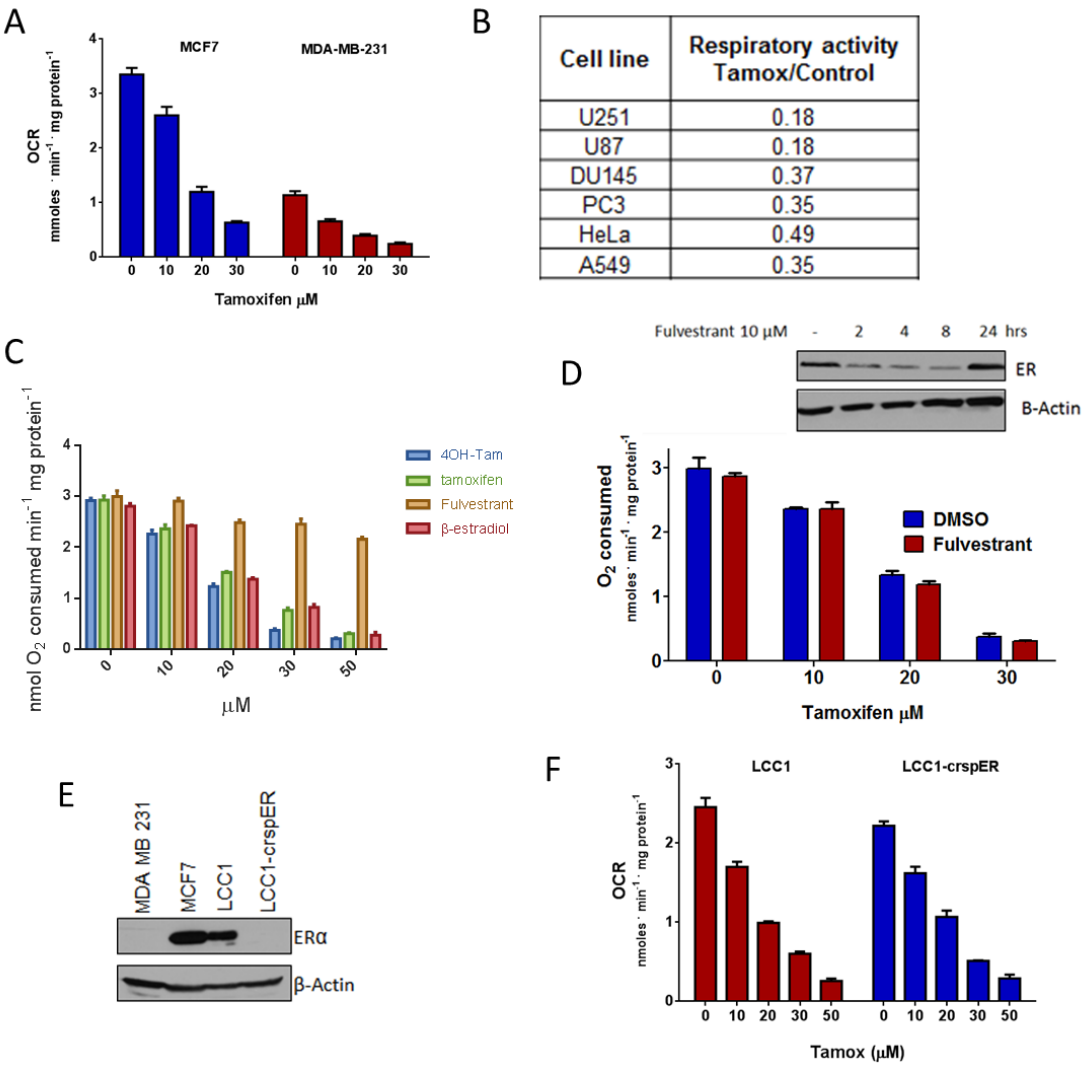

Cell line	Respiratory activity Tamox/Control
U251	0.18
U87	0.18
DU145	0.37
PC3	0.35
HeLa	0.49
A549	0.35

Figure II-1: Tamoxifen Inhibits cellular oxygen consumption in an ER independent manner. A. Cellular oxygen consumption measurements in response to increasing doses of tamoxifen in ER+ MCF7 cells and ER- MDA-MB-231 cells. **B**. Fraction of oxygen consumption rate remaining after tamoxifen treatment at 30μM in a panel of cancer cell lines. **C**. Oxygen consumption measurements of BC cells treated with increasing doses of tamoxifen, 4OH-tamoxifen, fulvestrant, or β-estradiol. **D**. Oxygen consumption measurements of MCF7 cells pretreated with fulvestrant or vehicle control plus increasing doses of tamoxifen. Insert: Immunoblot of ER expression following fulvestrant treatment. **E**. Cellular oxygen consumption measurements of LCC1 cells and LCC1 cells with CRISPR-Cas9 mediated deletion of ERα treated with increasing doses of tamoxifen. Data are the average of three independent experiments ±SEM, *P<0.05 **P<0.01 ***P<0.001.

To determine if the effect of tamoxifen on oxygen consumption was due to a direct interaction with mitochondria, we isolated mitochondrial from mouse liver. Tamoxifen inhibited oxygen consumption in the presence of complex I substrates glutamate and malate but not in the presence of complex II substrate succinate (Figure II-2A). To investigate if tamoxifen affected cancer mitochondria similarly to mitochondria isolated from healthy cells, we used digitonin to permeabilize MCF7 and MDA-MB-231 cells. Tamoxifen inhibited oxygen consumption of mitochondria by 60% in both permeabilized cell lines. As seen in liver mitochondria, respiration of cancer mitochondria could be rescued by supplementation with electron transport chain complex II substrate succinate but not with complex I substrates, glutamate and malate (Figures II-2B and II-2C). These effects of tamoxifen on mitochondria respiration are similar to what is seen with rotenone, a known complex I inhibitor. For experimental control we also determined that antimycin A, a complex III inhibitor, shuts down oxygen consumption in both permeabilized cell lines in the presence of succinate (Figures II-2B and II-2C). This indicates that the tamoxifen-mediated inhibition of oxygen consumption occurs through a direct effect on mitochondria, upstream of complex II. Interestingly, while intact MCF7 cells exhibit higher oxygen consumption rate than MDA-MB-231cells, this difference is lost once the cells are permeabilized. This may indicate that the higher rate of OXPHOS in MCF7 cells is due to a mechanism upstream of mitochondrial function. In addition, differing cell sensitivity to digitonin may play a role in the basal and succinate powered oxygen consumption rate. The addition of methyl succinate, a cell-permeable analog of succinate, reduced the ability of tamoxifen to inhibit oxygen consumption in intact BC cells (Figure II-2D) and significantly increased cell survival of MCF7 cells treated with tamoxifen (Figure II-2E). These results suggest that inhibition of

mitochondrial function upstream of complex II mediates the effects of tamoxifen on oxygen consumption and downstream effects.

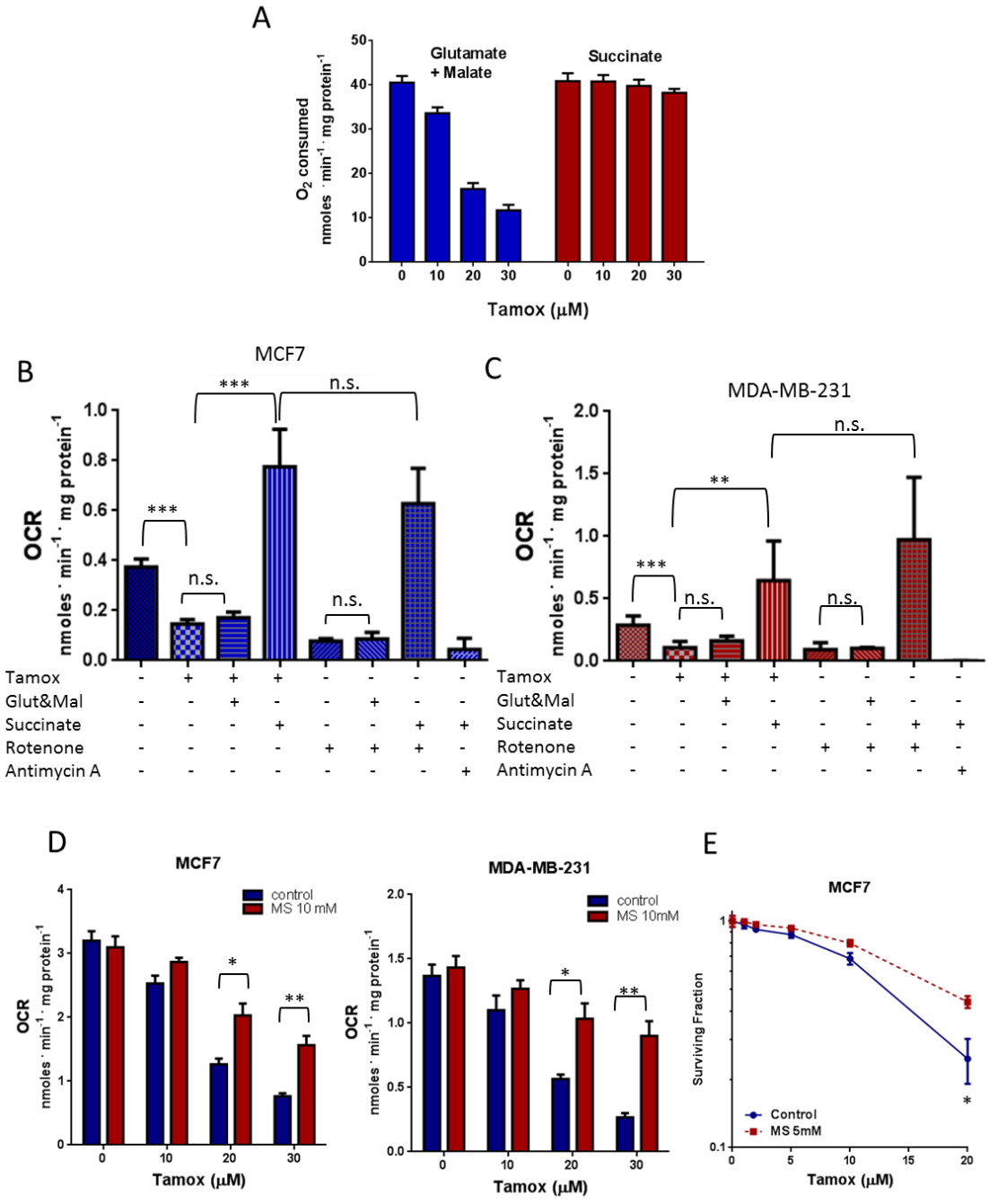

Previous Page - **Figure II-2: Tamoxifen inhibits oxygen consumption at mitochondrial complex I: A**. Oxygen consumption measurements of mitochondria isolated from mouse liver treated with tamoxifen in the presences of complex I or complex II substrates. **B**. Effect of tamoxifen on oxygen consumption of digitonin permeabilized MCF7 and **C**. MDA-MB-231 cells in the presence of complex I or complex II substrates compared to other mitochondrial electron transport inhibitors rotenone and antimycin A. **D**. Oxygen consumption measurements of MCF7 and MDA-MB-231 cells treated with Tamoxifen alone or in the presence of methyl succinate. **E**. Survival of MCF7 cells (N=6) treated with tamoxifen alone or in the presence of methyl succinate. Data are the average of three independent experiments ±SEM *P<0.05 **P<0.01. ***P<0.001.

Upon inhibition of oxygen consumption, it is expected that ATP synthesis via OXPHOS would be reduced resulting in accumulation of AMP. To determine if inhibition of oxygen consumption by tamoxifen alters cellular energy charge we quantified intracellular AMP and ATP pools following tamoxifen treatment. Tamoxifen increased the AMP:ATP ratio in MDA-MB-231 cells and MCF7 cells (Figure II-3A), the major activating mechanism of AMPK, as soon as 5 min after tamoxifen treatment and this ratio further increased following one hour of treatment. This increase in the AMP:ATP ratio correlated with a concomitant increase in tamoxifen- induced AMPK phosphorylation of the downstream signaling target acetyl-CoA carboxylase (ACC) and dephosphorylation of the mTOR targets 70 kDa ribosomal protein s6 kinase 1 (p70S6K), ribosomal protein s6 (pS6), and eukaryotic translation initiation factor 4E binding protein 1 (4EBP1), in both MCF7 (Figure II-3B) and MDA-MB-231 cells (Figure II-3C). To investigate if ER signaling is necessary for tamoxifen activation of the AMPK pathway, we used pharmacologic and genetic methods to block ER signaling. Pretreatment with fulvestrant to promote downregulation of the ER did not inhibit tamoxifen activation of AMPK (Figure II-3D). Furthermore, activation of AMPK in LCC1-crspER was comparable to that in LCC1 parental cells (Figure II-3E), indicating that the effects of tamoxifen on AMPK signaling were also ER-independent.

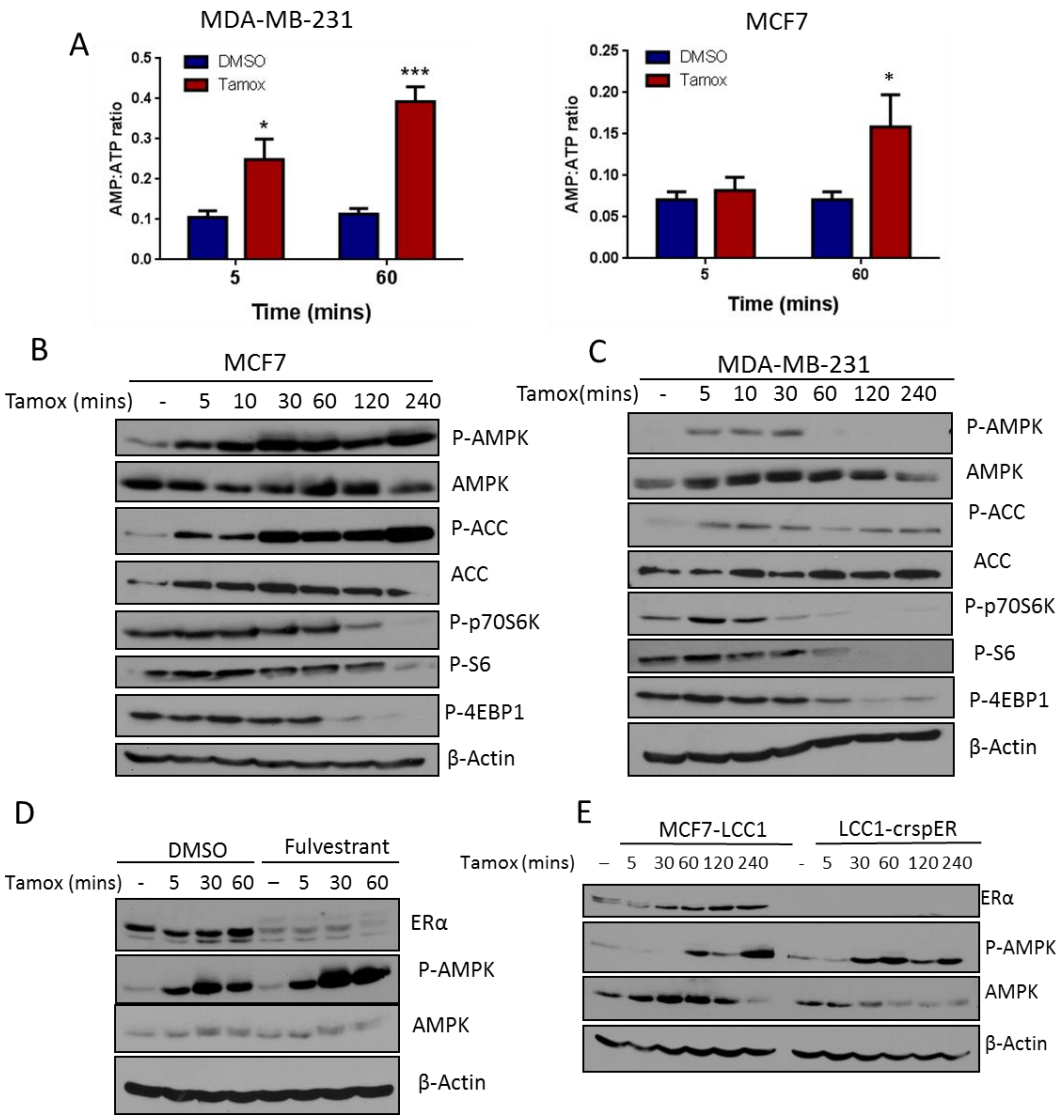

Figure II-3: Tamoxifen rapidly and acutely activates AMPK independently of estrogen receptor signaling. A. HPLC quantification of the AMP:ATP ratio in MDA-MB-231 (N=6) and MCF7 (N=3) cells treated with 30 μM tamoxifen for 5 and 60 mins, ±SEM *P<0.05 **P<0.01. **B**. Immunoblot of AMPK pathway activation following treatment with 30μM tamoxifen in MCF7 and **C**. in MDA-MB-231 cells. **D**. Immunoblot analysis of ER expression and AMPK activation in MCF7 cells treated with 10 μM fulvestrant or DMSO for 4 hrs preceding treatment with 30 μM tamoxifen over time. **E**. Immunoblot of AMPK activation in LCC1 cells and LCC1 cells with CRISPR-Cas9 deletion of ERα following tamoxifen treatment.

Upon an increase in the AMP:ATP ratio in the cell, AMP binds the gamma subunit of AMPK which results in a conformational change that stabilizes phosphorylation of the alpha subunit. Multiple AMPKα kinases have been reported, we focused on the two most well-known: LKB1 and CaMKK2 to investigate their role in AMPK activation upon tamoxifen treatment in BC cells. We used siRNA to knock down expression of LKB1 and CaMKK2 in both MCF7 and MDA-MB-231 cell lines. In MCF7 cells knock down of either LKB1 or CaMKK2 alone was not sufficient to prevent activation of AMPK**.** Concurrent knock down of both kinases was required to prevent AMPK phosphorylation (Figure II-4A). In MDA-MB-231 cells siRNA knock down of LKB1 alone did not prevent tamoxifen-mediated phosphorylation of AMPK, while knock down of CaMKK2 was sufficient to inhibit phosphorylation of AMPK upon treatment with tamoxifen (Figure II-4A). However, under CaMKK2 knock down, treatment with tamoxifen still resulted in phosphorylation of the AMPK target ACC, indicating that AMPK was still activated even without phosphorylation as detected by immunoblot. This is consistent with reports noting that AMP binding is enough to activate AMPK kinase[56]. Similar to MCF7 cells, In MDA-MB-231 cells, knockdown of both LKB1 and CaMKK2 prevented both AMPK phosphorylation and downstream signaling, as monitored by phosphorylation of the AMPK target ACC (Figure II-4A).

During the course of these experiments, no antibody was available that accurately detected CaMKK2 expression by immunoblot, therefore we could not confirm successful knock down by siRNA. To confirm the effects of CaMKK2 knock down of AMPK activation following tamoxifen treatment we used the CaMKK2 inhibitor STO609. As expected, treatment with this drug had no effect on tamoxifen-mediated AMPK phosphorylation in MCF7 cells but did prevent phosphorylation of AMPK following tamoxifen treatment in MDA-MB-231 cells (Figure II-4B). Thapsigargin was used as a

control for CaMKK2-mediated AMPK phosphorylation. As expected, treatment with STO609 prevented AMPK phosphorylation following Thapsigargin treatment (Figure II-4B). Overall, these results indicate that tamoxifen-mediated AMPK phosphorylation is mediated by multiple upstream AMPK-kinases and the extent of their importance is cell type specific.

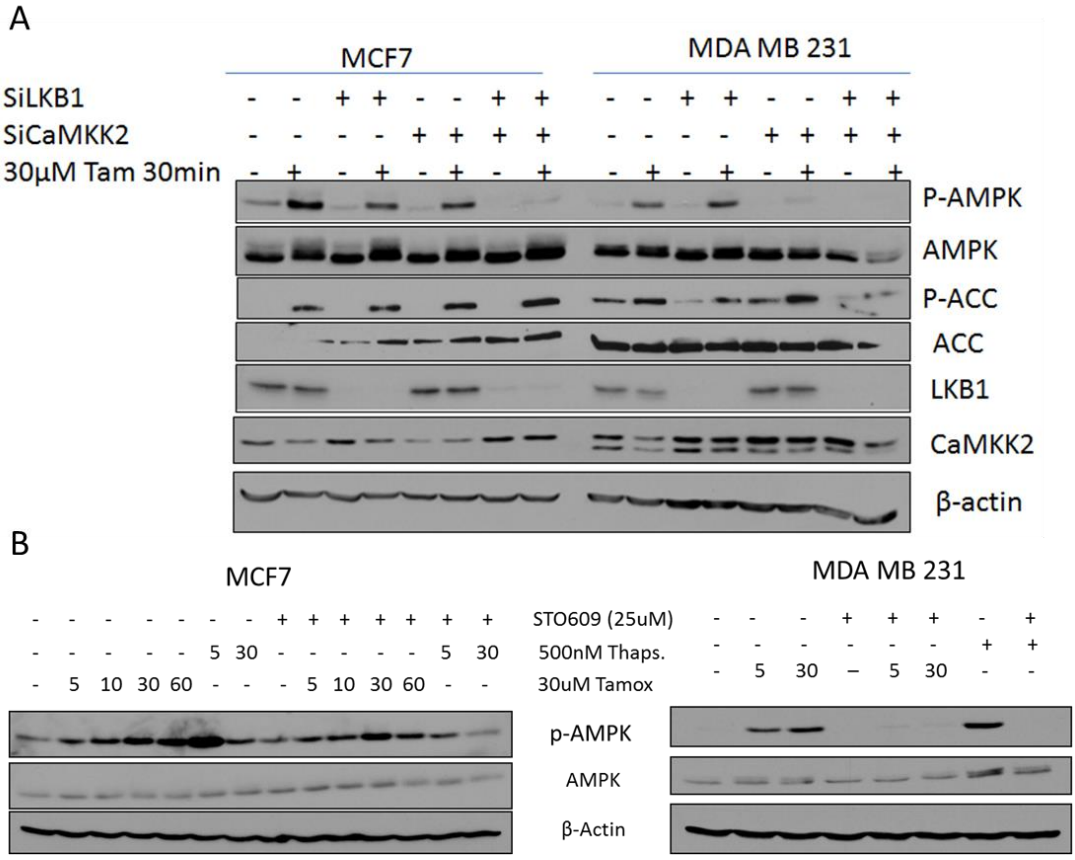

Figure II-4: LKB1 and CaMKK2 can both phosphorylate AMPK in response to tamoxifen. A. Immunoblot of AMPK pathway activation with tamoxifen after siRNA knock down of LKB1 and CaMKK2 in MCF7 and MDA-MB-231 cells. **B**. Immunoblot of the effect of CaMKK2 inhibitor STO609 on Tamoxifen activation of AMPK.

To further dissect the biological role of AMPK in the cellular response to tamoxifen, we used the CRISPR-cas9 system to knock out AMPKα1 in MDA-MB-231 cells. We observed that loss of AMPKα1 resulted in a compensatory increase in AMPKα2 expression (Figure II-5A) and induced an increased survival in response to tamoxifen treatment (Figure II-5B). This effect was recapitulated in MCF7 cells where AMPKα1 inhibition by shRNA resulted in reduced levels of cleaved PARP and increased survival upon tamoxifen treatment compared to shNT-transfected cells (Figures II-5C and II-5D). To evaluate the impact of complete inhibition of AMPK catalytic activity on cellular response to tamoxifen, we used siRNA to knock down AMPKα2 in both wild type MDA-MB-231 cells and in crspAMPKα1 cells. Loss of AMPKα2 in MDA-MB-231 cells resulted in increased cell death upon tamoxifen treatment whereas knockdown of AMPKα2 in the AMPKα1 CRISPR knockout cells resulted in further increase in tamoxifen-induced cytotoxicity (Figure II-5B). Notably, while the dual AMPKα1/2 knockdown showed the highest levels of tamoxifen toxicity as determined by the modified MTT assay, the levels of apoptosis markers cleaved poly-ADP ribose polymerase (PARP) and cleaved caspase 3 were quite low. This could be due to more rapid processing of these markers under these conditions as indicated by complete loss of total PARP in these cells. Interestingly, knockdown of either isoform of AMPKα resulted in loss of phospho-ACC upon tamoxifen treatment, while loss of AMPKα1 alone ameliorated the inhibition of the mTOR pathway following tamoxifen treatment. Induction of autophagy remained unchanged upon AMPKα1 inhibition; however, knockdown of both isoforms substantially reduced autophagy levels as seen by a reduction in microtubule-associated protein light chain 3 (LC3) processing (Figure II-5A)

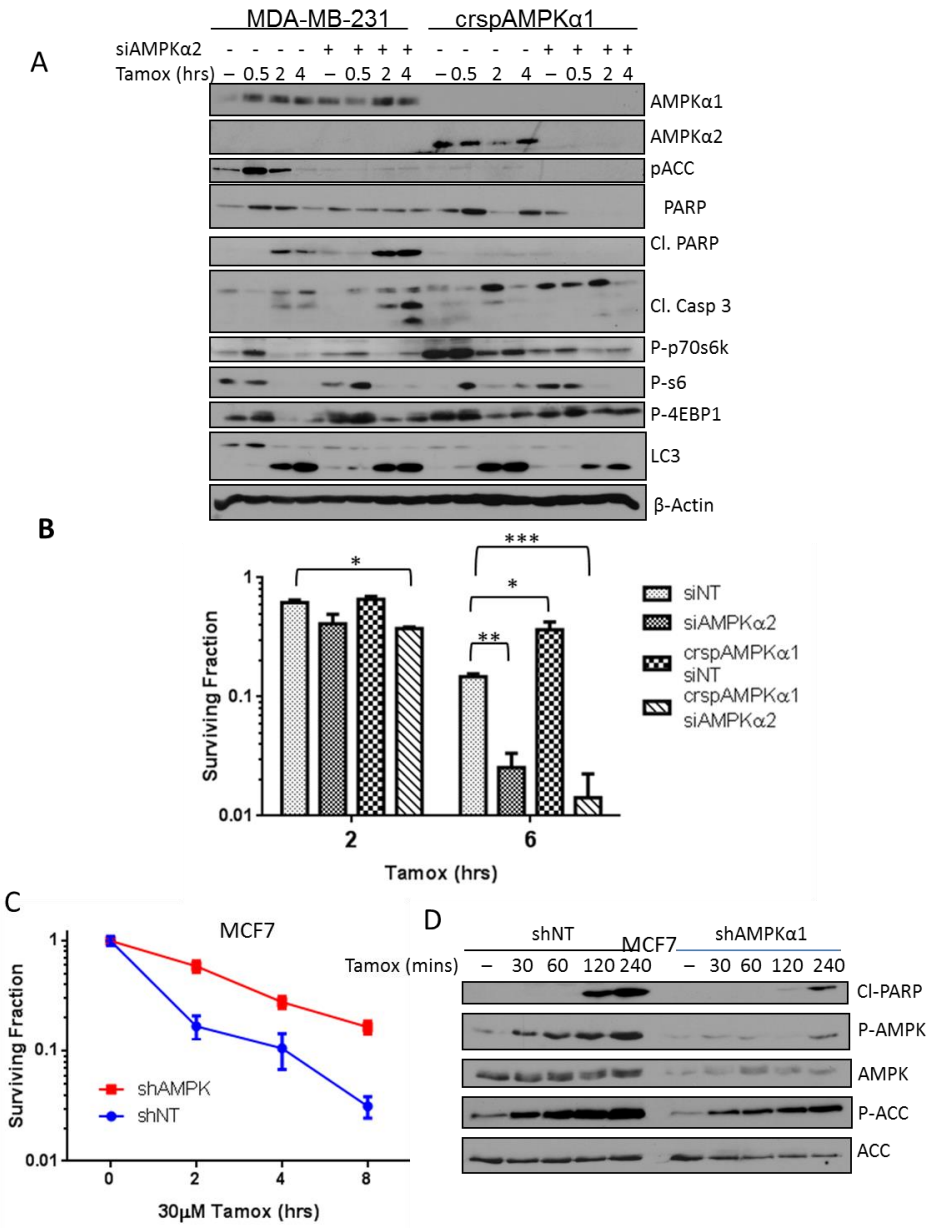

Figure II-5: AMPKα1 and AMPKα2 mediate divergent effects on downstream effectors and cellular survival after tamoxifen treatment. **A**. Immunoblot of AMPK pathway activation and apoptotic markers after tamoxifen treatment in MDA-MB-231 cells with CRSPR-cas9 knock out of AMPKα1 or siRNA knock down of AMPKα2. **B**. Modified MTT assay of survival of AMPK knock down cells treated with 30 μM tamoxifen for 4 hrs. **C**. Clonogenic survival of the effect of AMPK knockdown by shRNA in MCF7 cells treated with 30 μM tamoxifen. **D**. Immunoblot of AMPK activation and apoptotic markers following tamoxifen treatment of MCF7 cells transfected with shNT or shAMPKα1. Data are the average of three independent experiments ±SEM *P<0.05 **P<0.01 ***P<0.001

To further investigate the role of AMPK isoforms in the autophagic response of BC cells to tamoxifen treatment we pretreated cells with E64d and pepstatin A to prevent LC3-II recycling and monitored autophagic flux by immunoblot. While we saw reduced levels of LC3-II in both siAMPKα2 and crspAMPKα1 conditions, MDA-MB-231 cells require both AMPKα1 and AMPKα2 to be knocked down in order to significantly reduce autophagy induction with tamoxifen treatment (Figure II-6A). This data suggests that AMPK activation promotes autophagy in response to tamoxifen treatment.

To determine if the AMPK isoform-specific effects on the mTOR pathway impacted upon cellular translation, we pulse-labeled MDA-MB-231 cells and crspAMPKα1 cells with [^{35}S]-cysteine and methionine. Translation was inhibited in both cell lines, albeit to a substantially lesser extent in the crspAMPKα1 cells upon tamoxifen treatment (Figure II-6B and II-6C).

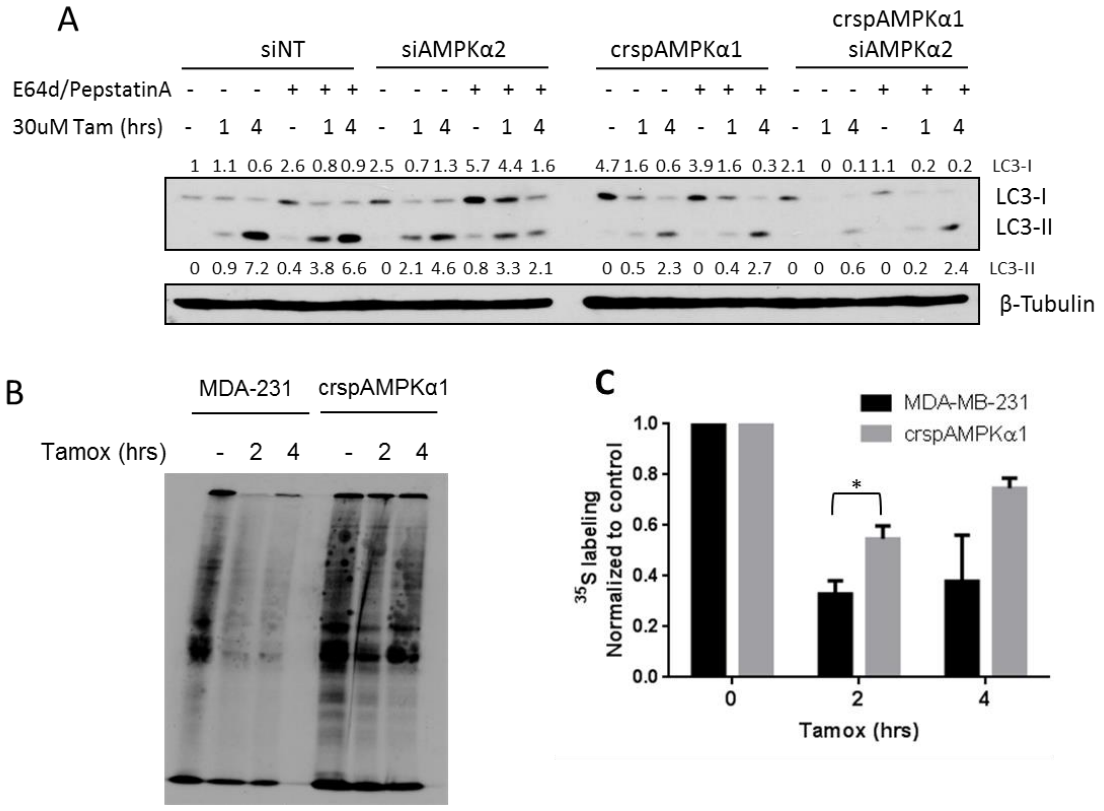

Previous page- **Figure II-6: AMPKα isoform specific effects on downstream pathway mediators**. **A**. Immunoblot of LC3-I and LC3-II flux with tamoxifen treatment as affected by AMPK status. Values represent Pixel intensity of LC3-I (top) or LC3-II (bottom) normalized to untreated control. **B.** Autoradiograph of ^{35}S incorporation into proteins following tamoxifen treatment in MDA-MB-231 cells or MDA-MB-231 cells with CRISPR-cas9 knock out of AMPKα1. **C**. Quantification of ^{35}S signal. Data are the average of three independent experiments ±SEM *P<0.05 **P<0.01 ***P<0.001.

To determine if tamoxifen activates the AMPK pathway *in vivo,* we injected 4175 cells, a variant of the MDA-MB-231 triple negative breast cancer cell line[57] into the mammary fat pad of athymic nude female mice. After 3 weeks of tumor growth, 100 mg/kg tamoxifen was administered once daily for 3 days. Mean tamoxifen and metabolite levels of 4-hydroxy-tamoxifen and N-desmethyl-tamoxifen quantified by LC-MS/MS in the tumor tissue were 19.07, 3.97 and 33.64 ng/mg respectively (Figure II-7A). This data indicates that the concentrations of tamoxifen needed to activate the AMPK pathway *in vitro* are achievable *in vivo*. Tumors in mice treated with tamoxifen also had significantly higher levels of phospho-AMPK and displayed downregulation of the mTOR target phospho-4-EBP1 (figure II-7B and II-7C). These results are in agreement with the tamoxifen-induced AMPK pathway activation seen *in vitro*.

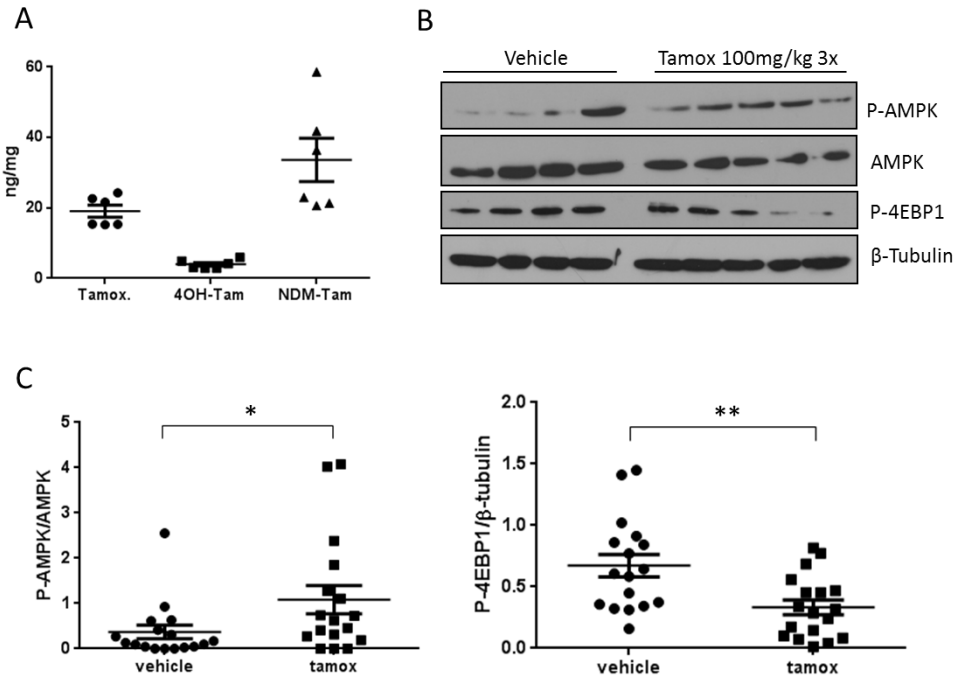

Figure II-7: Activation of the AMPK pathway by tamoxifen *in vivo*. A. Tamoxifen and its metabolite levels in tumor tissue from 6 representative lysates following treatment of nude mice bearing 4175 tumors with tamoxifen (100mg/kg) for 3 days analyzed by LC-MS/MS. **B**. Representative Immunoblot of AMPK pathway activation in tumor lysates. **C**. Densitometry analysis of signal intensity of Phos-AMPK normalized to total AMPK and Phos-4EBP1 normalized to β-Tubulin. Data is the average ±SEM of N=17 per group, *P<0.05 **P<0.01.

Discussion:

We have demonstrated that beyond its anti-estrogenic effects, tamoxifen exerts a pronounced and immediate effect on tumor metabolism via a non-ER, mitochondrial-specific pathway. Specifically, through the inhibition of oxygen consumption upstream of complex II, the increase in AMP/ATP ratio leads to activation of AMPK. We also discovered a previously unreported dichotomy in the role of AMPK isoforms in tumor survival following metabolic stress. Whereas AMPKα1 primarily appears to promote cell

death through inhibition of the mTOR pathway and translation, AMPKα2 promotes survival by a yet unidentified mechanism.

While the clinical benefit of tamoxifen in ER^+ breast cancer patients has been mainly attributed to inhibition of ER activity, tamoxifen has previously been shown to have multiple effects independent of ER. We have further characterized the effects of tamoxifen on mitochondria by describing the dose dependent effects on oxygen consumption to occur independent of ER. We have also demonstrated that AMPK activation occurs in both ER^+ and ER^- BC cells and that it is independent of ER signaling. In addition, tamoxifen activated the AMPK pathway in an orthotopic model of triple negative breast cancer. While we treated these animals for a short time at a high dose, we would anticipate similar effects at a lower dose over a longer period of time, as tamoxifen has been shown to accumulate in tumor tissues to levels up to 60-70 times the plasma concentration [21].

The non-ER dependent effects of tamoxifen described here, have the potential to expand the therapeutic window for tamoxifen into ER- BC and non-breast cancers. Furthermore, most ER+ BC related deaths have been attributed to metastatic disease which is often tamoxifen-resistant [6]. While the mechanism by which tamoxifen resistance occurs remains unclear, it is thought to involve alterations in ER itself and alterations in the levels of co-regulators or downstream effectors in the signaling pathway [6]. Our results suggest that it would be valuable to further explore whether combination therapies that take advantage of the metabolic effects of tamoxifen could restore tamoxifen sensitivity or prevent resistance.

The precise target for tamoxifen in the mitochondrial respiration chain is not currently clear. The evidence presented in this manuscript supports the hypothesis that tamoxifen inhibits complex I in the electron transport chain. The ability of the complex II

substrate succinate to restore oxygen consumption in tamoxifen treated cells points to the inhibition of mitochondrial respiration upstream of complex II. Moreover, the inability of complex I substrates glutamate and malate to restore any oxygen consumption in permeabilized BC cells indicates that complex I may be the site of tamoxifen action. However, we cannot completely rule out possible effects of tamoxifen on upstream processes, such as the TCA cycle, that contribute electron donors to the respiratory chain. Another implication of our findings with translational potential is the fact that inhibition of oxygen consumption is a validated strategy to increase tumor pO2 and decrease hypoxia, a major cause of cancer resistance to genotoxic therapy, including radiation[46]. Therefore, tamoxifen has the potential to function as a radiation and chemotherapeutic sensitizer. In fact, other complex I inhibitors, such as metformin, have shown anti-cancer effects through both their metabolic effects and activation of AMPK[42,58]. Although our results are reminiscent of the metabolic effects of metformin treatment, both the inhibition of oxygen consumption and activation of AMPK occur at a far more rapid rate (5-10 mins) than that seen with metformin (12-24 hrs). It is also important to note that while *in vitro* metformin exerts its OXPHOS-inhibitory effects at doses ranging from 1-50 mM, tamoxifen does so at low μM concentrations.

The anti-tumorigenic effects of metformin in BC have been shown to be dependent on its activation of AMPK [58]. We asked if AMPK had a similar role in BC survival of tamoxifen treatment. We used the CRISPR-cas9 system to delete AMPKα1 from MDA-MB-231 cells and observed a compensatory increase in AMPKα2 expression. This would lead us to hypothesize that the isoforms have redundant effects, yet, we observed opposing effects on cell survival. Other work examining the isoforms of AMPKα has identified some differences, AMPKα2-/- mice exhibit mild insulin resistance

and impaired glucose tolerance while AMPKα1-/- mice do not have a detectable metabolic phenotype[59,60] . At the molecular level, AMPKα2 has been shown to be more reactive to AMP and is able to localize to the nucleus[61]. Moreover, AMPKα2 expression has been shown to be suppressed in primary BC[62]. In our system, knock out of AMPKα1 alone rescued cells from tamoxifen treatment while knock down of AMPKα2 increased cell death. Immunoblot analysis and [^{35}S] labeling of proteins indicated that the α1 subunit is responsible for downregulation of the MTOR pathway and translation. However, both isoforms are needed to inhibit ACC and either isoform can activate autophagy. We suspect that it is the loss of robust autophagy induction in the dual AMPKα1α2 knockdown that results in increased tamoxifen cytotoxicity under those conditions. The ability of tamoxifen to activate autophagy is well established[63,64] however, the data reported here is the first to directly identify AMPK activation as a mechanism of autophagy induction in tamoxifen treated BC cells.

In summary, we have described the ability of tamoxifen to inhibit oxygen consumption via an ER-independent direct effect of mitochondria, upstream of complex II. We have also shown that tamoxifen treatment results in robust AMPK activation and identified AMPK as a mediator of tamoxifen toxicity through isoform specific effects.

CHAPTER 3: Characterization of the effects of tamoxifen on glucose and fatty acid metabolism and exploitation of the metabolic effects of tamoxifen for therapeutic opportunities.

Sections of this chapter contribute to the published manuscript:

Natalie A. Daurio, Stephen W. Tuttle, Andrew J. Worth, Ethan Y. Song, Julianne M. Davis, Nathaniel W. Snyder, Ian A. Blair, and Constantinos Koumenis. **AMPK activation and metabolic reprogramming by tamoxifen through estrogen receptor-independent mechanisms suggests new uses for this therapeutic modality in cancer treatment.** *Cancer Res* OnlineFirst March 28, 2016.

Introduction:

Tamoxifen treatment has been reported to affect multiple metabolic processes. These have included inhibition of mitochondrial function[22,65,66], increased FDG-PET signaling following treatment[67–69], and altered lipid homeostasis including decreased cholesterol levels[4] and increased incidence of non-alcoholic fatty liver disease[70]. We have shown that tamoxifen mediated inhibition of oxidative phosphorylation results in metabolic stress characterized by an increase in AMP/ATP ratio and activation of the AMPK pathway. Activation of AMPK functions to rebalance cellular energy charge by turning off ATP consuming processes, including protein and fatty acid synthesis, and turning on ATP generating processes such as glycolysis, autophagy and fatty acid oxidation. As a result AMPK activation results in a significant reprogramming of cellular metabolic processes. AMPK activation promotes glycolytic activity by increasing glucose uptake through transporters GLUT1[71] and GLUT4 and activates glycolytic enzymes by increased transcription of hexokinase II and direct phosphorylation of phosphofructiokinase[48,50]. AMPK also shifts fatty acid metabolism from synthesis to oxidation. This occurs through the phosphorylation and inhibition on acetyl CoA carboxylase (ACC) the first committed step of fatty acid synthesis and through decreased activity of SREBP1a, the transcription factor that controls gene expression of many lipogenic enzymes including FASN, sterol-CoA desaturase 1 (SCD1) and glycerol-3-phosphate acetyltransferase (GPAT)[48,50].

In terms of metabolic targeted therapies, it has been postulated that concurrently targeting adaptive responses to metabolic reprogramming can lead to significant enhancement of the therapeutic window for multiple chemotherapeutic modalities[72,73]. Therefore the combination of tamoxifen with other metabolically targeted agents may

have therapeutic value. Moreover, oncogene activation results in increased dependence on upregulated metabolic pathways. For example, both BRAF and KRAS mutations promote glycolysis[44,74]. Resistance to targeted therapies limits the therapeutic options in cancers such as melanoma and pancreatic cancer that are driven by these pathways. The drug resistant populations are thus dependent on elevated OXPHOS and drugs that target mitochondrial metabolism, including metformin, have potential utility in targeting such resistant populations by synthetic-lethality approaches[38,40,43,44].

Here, we characterize the changes in cellular metabolism that occur with tamoxifen treatment. We show that tamoxifen treatment up regulates glucose uptake and glycolysis and concurrent treatment with tamoxifen and glycolytic inhibitors result in increased cell death. We also characterize the effects of tamoxifen on fatty acid metabolism. In addition, we demonstrate that tamoxifen treatment is toxic to OXPHOS addicted cancer cell populations.

Results:

AMPK activation is known to increase glycolytic activity in an attempt to restore cellular ATP pools[47]. To investigate if this occurred following tamoxifen treatment, we measured glucose uptake from the media in MDA-MB-231 and MCF7 cells. Glucose uptake increased in a dose-dependent manner with tamoxifen treatment in both cell lines (Figure III-1A). To examine if glycolysis was also upregulated by tamoxifen we analyzed the incorporation of [^{13}C] from [$^{13}C_6$]-Glucose into acetyl-CoA and lactate by LC-MS/MS. Following tamoxifen treatment we observed an increase in [^{13}C] labeling in these products, indicating an increase in glycolytic activity (Figure III-1B and III-1C). The activation of AMPK (P-AMPK) was enhanced under glucose deprivation conditions

(figure III-1D) and treatment with the glycolytic inhibitor 2-deoxyglucose (2DG) (figure III-1E) in both MCF7 and MDA-MB-231 cells, underscoring the importance of the glycolytic switch for ATP generation during tamoxifen treatment.

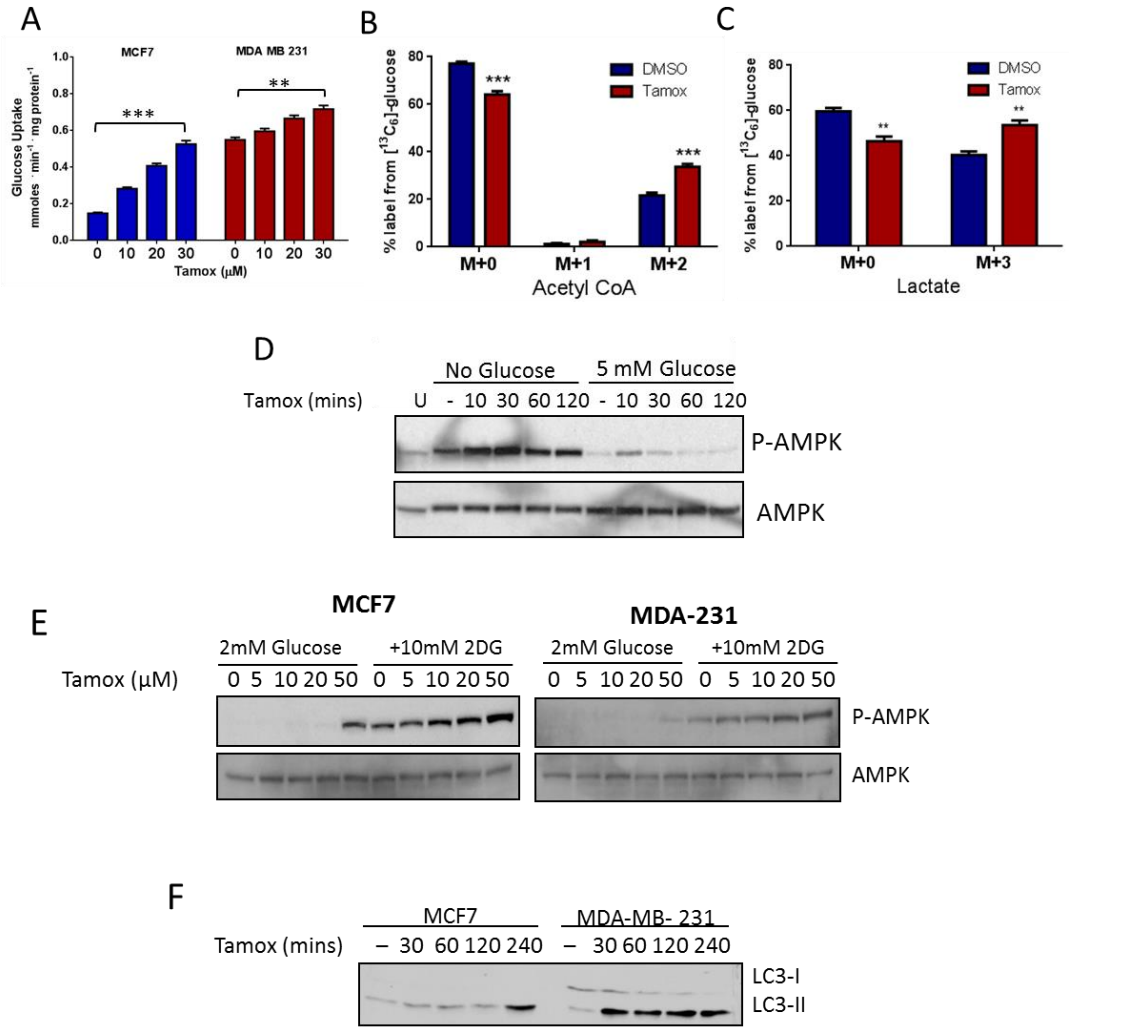

Figure III-1: Tamoxifen treatment promotes glycolysis. A. Glucose uptake from media following tamoxifen treatment for 1 hour in MCF7 and MDA-MB-231 cells. LC-MS/MS analysis of ^{13}C6-glucose metabolites after 30μM tamoxifen treatment for 1 hour in MDA-MB-231 cells: Mass isotopomer analysis of **B**. Acetyl CoA and **C**. Lactate. N=4, **P<0.01 ***P<0.001. **D**. Immunoblot analysis of phos-AMPK and total AMPK of cells treated with 20μM tamoxifen over time under glucose deprivation or 5mM glucose. **E**. Immunoblot analysis of P-AMPK and total AMPK of cells treated with 20μM tamoxifen over time +/- 2DG. **F**. Immunoblot analysis of LC3-I and LC3-II in BC cells after tamoxifen treatment.

To investigate if glucose metabolism via the TCA cycle was altered with tamoxifen treatment we looked at [$^{13}C_6$]-Glucose labeling of TCA cycle intermediates citrate (Figure III-2A), malate (Figure III-2B), and succinyl-CoA (Figure III-2C). We observed a very small increase in the labeled fraction of citrate and succinyl-CoA but not of malate. While this data is statistically significant, the increase is very minor and is likely not physiologically significant and indicates that glucose metabolism through the TCA cycle is not changed with tamoxifen treatment. In addition to entering the TCA cycle, the acetyl-CoA that is created from glucose as an end product of glycolysis can also enter fatty acid metabolism pathways through conversion to malonyl-CoA by the enzyme ACC. ACC is an AMPK target and phosphorylation of ACC by AMPK inhibits enzyme function. ACC is the main AMPK target responsible for reduction of fatty acid synthesis upon loss of intracellular ATP. We analyzed [^{13}C]6-Glucose label incorporation into malonyl-CoA following tamoxifen treatment and observed an increase in labeled fraction in tamoxifen treated cells (Figure III-2D) indicating that a larger amount of malonyl-CoA is derived from glucose following tamoxifen treatment. These results were unexpected, given that AMPK activation should reduce malonyl-CoA synthesis. However, with a large increase in glycolytic activity upon tamoxifen treatment it is possible that the increase in malonyl-CoA labeled fraction from glucose is due to substrate excess.

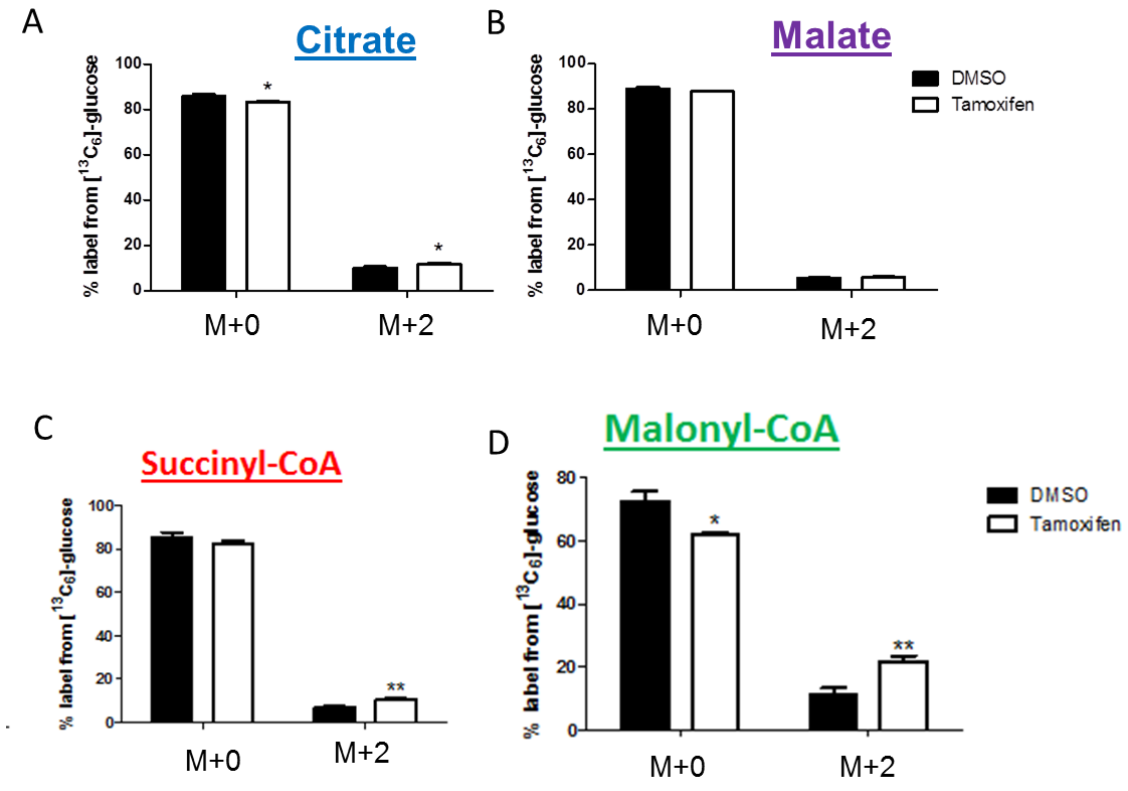

Figure III-2: ^{13}C6-Glucose labeling of TCA cycle intermediates and malonyl-CoA. Isotopomer analysis by LC-MS/MS of [$^{13}C_6$]-glucose label incorporation into **A**. Citrate **B**. malate **C**. succinyl-CoA and **D**. malonyl-CoA. Data are the average of four independent experiments ±SEM *P<0.05 **P<0.01 ***P<0.001.

Since we demonstrated that tamoxifen blocks OXPHOS and concurrently increases glucose uptake and utilization, it is likely that effective strategies for metabolic targeted therapies may require the inhibition of both OXPHOS and glycolysis simultaneously. 2DG, a non-metabolisable analog of glucose and 3-Bromopyruvate (3BP), an alkylating agent and inhibitor of hexokinase-2 and glyceraldehyde 3-phosphate dehydrogenase (GAPDH), induced a dose-dependent decrease in glucose uptake, as expected (Figure III-3A and III-3C). More importantly, combined treatment with relatively non-toxic doses of each of these inhibitors with tamoxifen significantly

enhanced tamoxifen-induced cytotoxicity in MCF7 cells and in MDA-MB-231 cells (Figures III-3B and III-3D). Notably, the sensitization to tamoxifen was larger in the MDA-MB-231 cells, which display a higher basal rate of glucose uptake (Figure III-3A) and lower basal level of OXPHOS (Figure II-1A).

We then tested if combination of tamoxifen with glycolytic inhibitors were effective in reducing tumor growth in an in vivo model of triple negative breast cancer. The MDA-MB-231 variant 4175 cells were injected orthotopically into the mammary fat pad. Mice were randomized into four groups: vehicle control, tamoxifen only, 3BP only and tamoxifen plus 3BP. Two weeks after tumor implantation, mice were given a loading dose of tamoxifen, followed by a maintenance dose of 25 mg/kg every 3 days. 3BP was given daily at 5mg/kg. Tumor growth was monitored twice weekly for 35 days. While the treatment was tolerable, no difference in tumor growth was seen between any treatment groups and control mice (Figure III-3E). Multiple factors may be responsible for the lack of efficacy seen in this model. Dose limiting toxicity of 3BP was significant; therefore, it may be that the tolerable dose was not high enough to reduce glycolysis in the tumor. Moreover, tumor growth in this model is quite slow, and may be that the metabolic stress induced by this treatment combination would be effective in a more aggressive model.

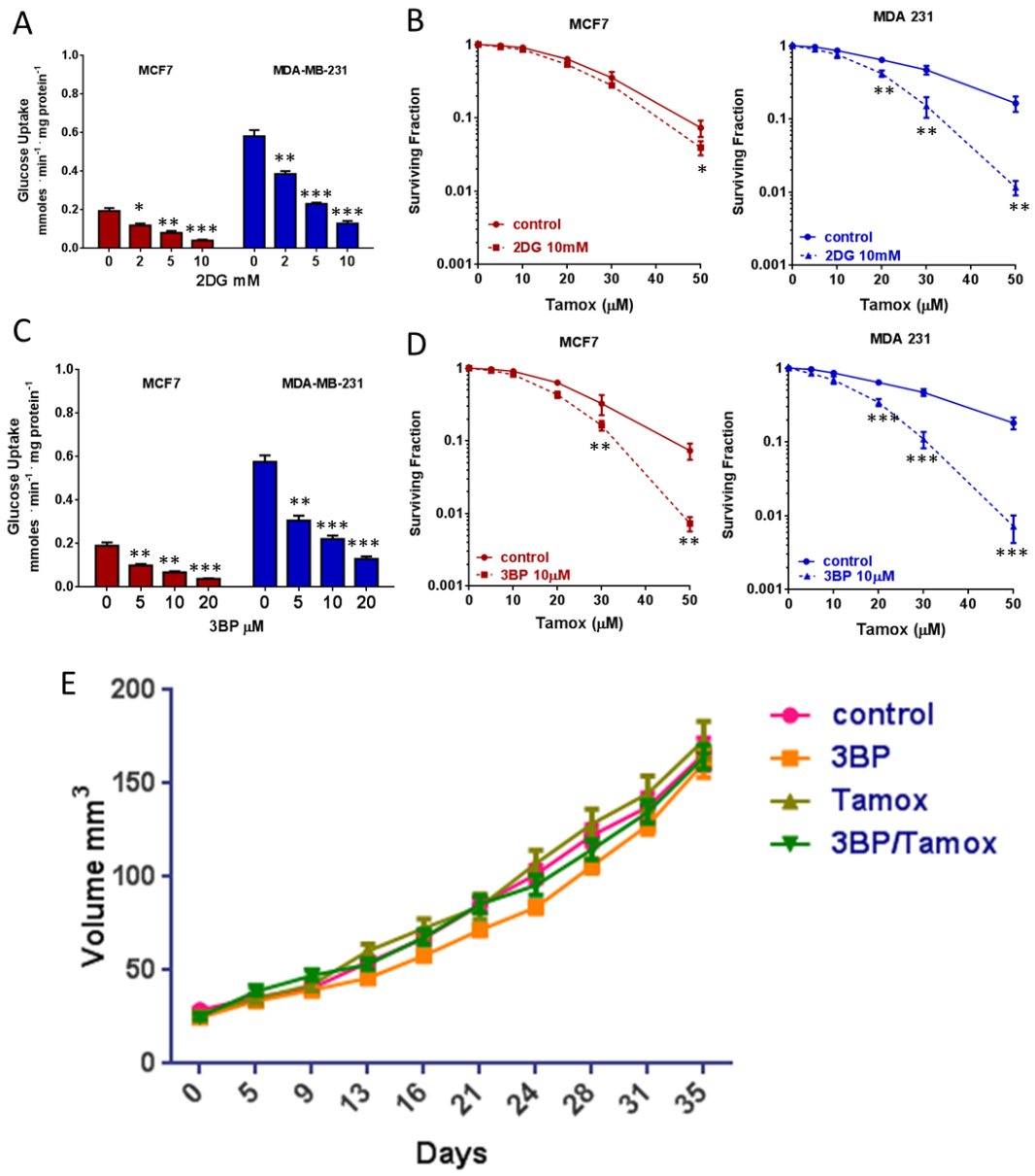

Figure III-3: Tamoxifen treatment synergizes with glycolysis inhibitors. A. Glucose uptake measurements in BC cells treated with 2DG. **B**. Survival of BC cells treated with 2DG and tamoxifen or tamoxifen alone. **C**. Glucose uptake measurements in BC cells treated with 3-BP. **D**. Survival of BC cells treated with 3-BP and tamoxifen or tamoxifen alone. Data are the average of three independent experiments ±SEM *P<0.05 **P<0.01 ***P<0.001. **E**. Measurements of 4175 tumor volume ±SEM over time in in nude mice treated with vehicle control, 3BP only, Tamoxifen only, or both 3BP and Tamoxifen. N=20 per group.

Synthesis of fatty acids (FAs) which begins with the synthesis of malonyl-CoA from acetyl-CoA, are of particular importance in cancer due to the need to generate excess membranes for rapid proliferation. Moreover, the oxidation of FAs in the mitochondria can replenish cellular ATP levels during times of metabolic stress[75]. To examine if tamoxifen impacted FA metabolism, we performed metabolite analysis of fatty acyl-CoA species by LC-MS/MS. The analysis showed an accumulation of acetyl-CoA and malonyl-CoA following tamoxifen treatment (Figure III-4A). We also observed a reduction in succinyl-CoA and other medium chain acyl-CoA species (C3:0, C6:0) consistent with reports of the effects of other complex I inhibitors[76] and an accumulation of longer chain (C16-C20) acyl-CoA species (Figure III-4A). The addition of [^{13}C]-glucose or [^{13}C]-glutamine resulted in no labeling of the long-chain CoA metabolites, indicating that these fatty acyl-CoAs are not synthesized from glucose or glutamine *de novo* in response to tamoxifen treatment. It has been reported that under metabolic stress, cells switch from glucose and glutamine to acetate as a carbon source for fatty acid synthesis[77]. Indeed, upon tamoxifen treatment, labeling from [^{14}C]-acetate of the cellular lipid fraction increased (Figure III-4B).

Activation of the AMPK pathway is also known to promote β-oxidation of fatty acids as a strategy to increase ATP pools. The degradation of lipid droplets by autophagy, termed lipophagy, increases the supply of free FAs which are then transported into the mitochondria for oxidation[75]. We also observed a rapid activation of autophagy upon tamoxifen treatment (Figure III-1F). BODIPY 493/503 stain, which measures total neutral lipid content in the cell, decreased in cells treated with tamoxifen (Figure III-4C). These data suggest that the accumulation of the long chain acyl-CoA species results from breakdown of lipid droplets.

To further probe the role of fatty acid metabolism in the cellular response to tamoxifen treatment we supplemented the cell culture media with oleic acid conjugated BSA. Supplementation with oleic acid completely rescued MDA-MB-231 cells from tamoxifen cytotoxicity (Figure III-4D). Moreover, oleic acid restored mTOR activity as determined by immunoblot (Figure III-4E). However, oleic acid supplementation was not sufficient to inhibit AMPK phosphorylation upon tamoxifen treatment.

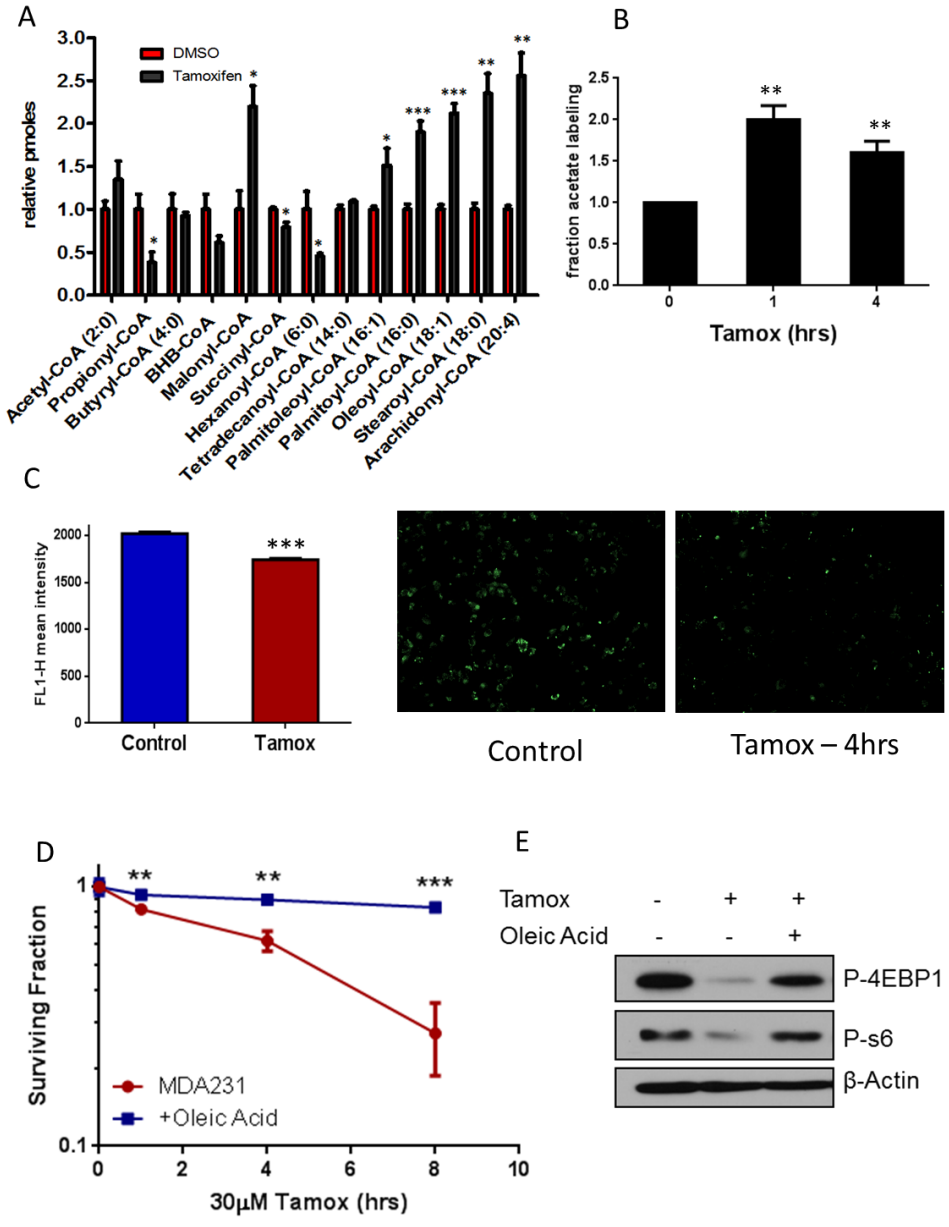

Previous page-**Figure III-4: Tamoxifen alters fatty acid metabolism: A.** LC-MS/MS metabolomic analysis of acyl-CoA species in MDA-MB-231 cells with and without tamoxifen treatment. **B**. quantification of ^{14}C-acetate radiolabel incorporation into total cellular lipid fraction. **C**. Flow cytometry quantification of BODPIY 493/503 stain intensity and representative images of BODIPY staining in control and tamoxifen treated MDA-MB-231 cells. **D**. Effect of oleic acid supplementation on the survival of MDA-MB-231 cells treated with tamoxifen. **E**. Immunoblot of the effect of oleic acid supplementation on tamoxifen inhibition of the mTOR pathway in MDA-MB-231 cells. Data is the average of three independent experiments +/- SEM. *P<0.05, **P<0.01, ***P0.001.

Acquired resistance to BRAF inhibitors in melanoma was recently shown to elevate oxygen consumption rate in the resistant cell population[40]. Therefore, we tested the effects of tamoxifen as a treatment in an *in vitro* model of OXPHOS addiction in cancer. We confirmed the previously reported increase in oxygen consumption rate in melanoma cells WM9 and 1205Lu selected over 3 days for a population that was resistant to the BRAF inhibitor PLX4720 (Figure III-5A and III-5B). We observed that tamoxifen inhibited oxygen consumption in this resistant population as well as the parental melanoma cell lines (Figure III-5A and III-5B). Tamoxifen induced cytotoxicity was then determined in the PLX4720 resistant population and the parental melanoma cell lines. The PLX4720-resistant population was more sensitive to tamoxifen (Figure III-5C and III-5D). Collectively, this data strongly suggests that tamoxifen can be used in combination with other therapies to effect robust anti-tumor effects via metabolic stress.

Next Page - **Figure III-5: Tamoxifen inhibits OXPHOS and is cytotoxic to BRAF-Inhibitor resistant melanomas.** BRAF mutant melanoma line WM9 and 1205Lu were treated with BRAF inhibitor PLX4720 for three days to select for a resistant population. **A**. Oxygen consumption measurements of the PLX4720 resistant population and the parental melanoma cell lines WM9 and **B**. 1205Lu treated with tamoxifen. **C**. Survival of the PLX4720 resistant population and the parental melanoma cell lines WM9 and **D**. 1205Lu treated with tamoxifen. Data is the average of three independent experiments +/- SEM. *P<0.05, **P<0.01, ***P0.001.

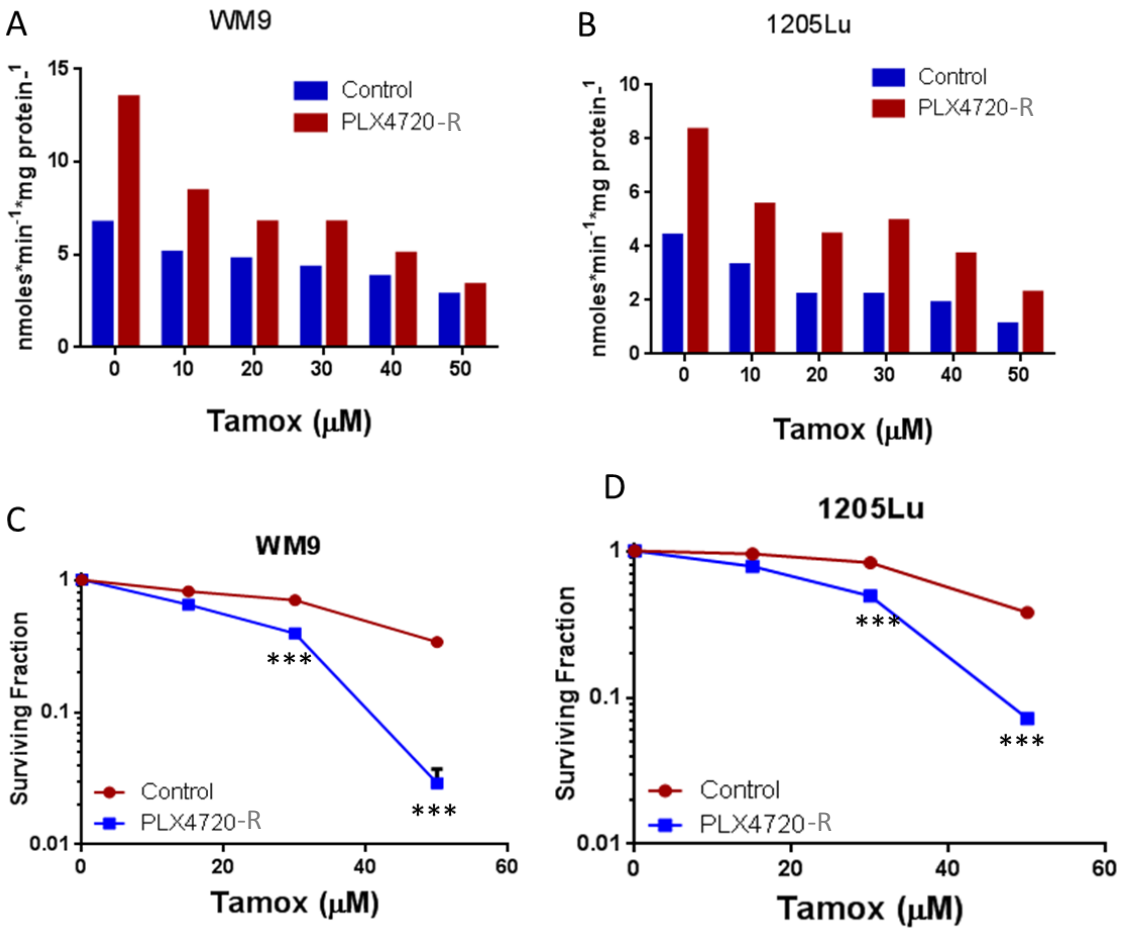

Discussion:

We have demonstrated that tamoxifen treatment increases glycolysis and cellular dependence on glycolytic activity for cell survival. This can be exploited for therapeutic benefit via combination treatment with tamoxifen and glycolytic inhibitors. We have also shown that tamoxifen alters cellular fatty acid metabolism through inhibition of fatty acid synthesis and depletion of intracellular lipid stores. Supplementation with fatty acids can

rescue cells from tamoxifen treatment, highlighting the importance of fatty acid oxidation under tamoxifen treatment conditions.

Tamoxifen inhibition of oxygen consumption results in an increase in the cellular AMP:ATP ratio and the activation of the AMPK signaling pathway and an increase in glycolytic activity. Other activators of AMPK, such as metformin, have also been shown to increase dependence on glycolysis. Intriguingly, soon after BC patients begin treatment with tamoxifen, a "metabolic flare" is often seen in their FDG-PET scans[67,69]. Although the cause for this radiologic abnormality has not been clearly delineated, it is reasonable to hypothesize that this could be due to increased uptake of FDG in response to metabolic reprogramming and AMPK activation, since GLUT 1 transporters, the major transporter system of glucose and FDG uptake, are AMPK targets[71].

We have also demonstrated the potential for increased therapeutic benefit through drug combinations with tamoxifen that have a synergistic effect via blockade of upregulated metabolic pathways. Glycolytic inhibitors have long been attractive clinical agents due to the Warburg effect, yet systemic toxicity has limited their success in the clinic. 2DG has been tested in clinical trials and 3BP has shown significant preclinical potential[78] .Our data suggests that clinical use of these inhibitors in combination with tamoxifen may result in increased efficacy and use of reduced doses that may limit toxicity.

While tamoxifen synergized with glycolytic inhibitors *in vitro*, combined treatment with tamoxifen and 3BP did not impact tumor growth in an *in vivo* model of triple negative breast cancer. The lack of efficacy *in vivo* may be due to multiple factors. First, 3BP is quite toxic and it is possible that the tolerated dose was not high enough to significantly reduce glycose metabolism in tumors. Tamoxifen has also been reported to inhibit of angiogenesis[79] which may further reduce drug delivery to the tumor. Tamoxifen,

a highly lipophilic drug, was delivered in peanut oil. Our *in vitro* data has shown that supplementation with fatty acids can rescue cells from tamoxifen cytotoxicity. Therefore, using lipids as the drug vehicle may have countered the effects of tamoxifen treatment or available fatty acids from circulation or tumor microenvironment may have also contributed to the lack of efficacy. Another possible explanation for the lack of in vivo efficacy may be the chosen tumor model. Rodent triple negative BC models progress quite slowly and it may be that the tumor can tolerate more metabolic stress due to low proliferation rate. It would be worthwhile to test the combination of tamoxifen and glycolytic inhibition in a more aggressive tumor model.

Our results are also in agreement with other metabolic effects of tamoxifen in patient populations. Women on tamoxifen therapy have an increased risk for developing non-alcoholic fatty liver disease[70]. However, the effects of tamoxifen on tumor fatty acid metabolism have not been investigated in detail. Accumulation of malonyl-CoA following tamoxifen treatment has been previously reported[80] and we also observed this in BC cells. The synthesis of malonyl-CoA is the rate-limiting step in fatty acid synthesis, thus its accumulation leads us to suspect that there is a decrease in the activity of FASN which is consistent with AMPK activation. It is also possible that increased upstream flux, through glycolysis and acetate utilization, contributes to the accumulation of malonyl-CoA with tamoxifen treatment. It is worth noting that AMPK is also known to inhibit fatty acid synthesis and promote β-oxidation, primarily through inhibiting ACC[47]. Metabolic labeling indicates that acetate and not glucose or glutamine functions as the carbon source for fatty acid synthesis during tamoxifen treatment. The propensity for cells to switch to acetate utilization under metabolic stresses including hypoxia and nutrient deprivation has been previously reported[77] and it is not surprising that it occurs under tamoxifen-generated metabolic stress as well.

Depletion of intracellular lipid stores and accumulation of long chain fatty acyl-CoAs are consistent with an increase in beta oxidation which is also expected under AMPK activation conditions. Due to the robust activation of autophagy we previously described under tamoxifen treatment we suspect that lipophagy plays a significant role in replenishing or maintaining ATP during metabolic stress via the release of free fatty acids from lipid droplets[75]. It is important to note that β-oxidation generates both NADH and $FADH_2$. Under conditions of complex I inhibition, the FADH2 generated via oxidation of fatty acids could feed into electron transport via complex II, similar to what is seen with the addition of succinate, to power ATP synthesis. The ability of oleic acid to rescue translation as well as survival highlights the dependence of tamoxifen treated BC cells on fatty acid metabolism for survival.

Interestingly, malonyl-CoA is known to inhibit carnitine palmitoyltransferase (CPT-1), the transporter responsible for transporting free fatty acids into the mitochondria for β-oxidation. As a result, it would be expected that β -oxidation would be decreased under tamoxifen treatment conditions due to the large accumulation of malonyl-CoA. Therefore it is possible that the ability of oleic acid to rescue tamoxifen treatment is not due to providing a substrate for ATP generation via β-oxidation but through providing fatty acids for membrane generation as tamoxifen has been reported to accumulate in lipid bilayers and likely damage cellular membranes. More experiments would be required to investigate the effects tamoxifen has on cellular membranes and whether oleic acid supplementation contributes to membrane repair.

Recognition of cancer as a heterogeneous disease has led to the development of personalized medicine and targeted therapies. Drugs designed to inhibit specific activated oncogenes often have early success, but are plagued by the emergence of resistance. If the pathways that contribute to resistance can be identified and inhibited, it

is reasonable to infer that resistance may be prevented or delayed. Resistance to BRAF and KRAS target therapies has been described to require increased dependence on OXPHOS. Our data shows that tamoxifen mediated inhibition of OXPHOS in this resistant population results in increased cell death. Therefore, the combination of tamoxifen with these targeted therapies may increase clinical response.

In conclusion, we have characterized the impact of tamoxifen treatment on glucose and fatty acid metabolism. These metabolic changes highlight pathways that may be essential for cell survival of tamoxifen treatment. We have demonstrated that glycolytic activity is required in tamoxifen treated cells and combination of tamoxifen and glycolytic inhibitors may be an effective therapeutic strategy. Additional *in vivo* models would be necessary to further test this hypothesis. Moreover, OXPHOS addiction is characteristic of resistance to BRAF and KRAS targeted therapies and tamoxifen inhibition of respiration is preferentially cytotoxic to this population and may be of clinical use to overcome resistance.

CHAPTER 4: Conclusions and Future Directions

Chapters II and III collectively describe a novel mechanism of action for tamoxifen, an extensively used drug for ER+ BC treatment (Figure IV-1). Tamoxifen inhibits oxygen consumption at complex I of the mitochondrial respiratory chain resulting in a decrease in oxygen consumption and increase in the intracellular AMP/ATP ratio. AMPK activation impacts cell survival through isoform specific downstream signaling. Tamoxifen treatment also results in an increase in glycolysis as well as alterations in fatty acid metabolism including break down of neutral lipid droplets, accumulation of long chain fatty acyl-CoAs, and an increase in acetate utilization (Figure IV-1). These metabolic effects of tamoxifen suggest strategies by which clinical efficacy may be increased through synergy with pharmacological targeting of upregulated metabolic pathways.

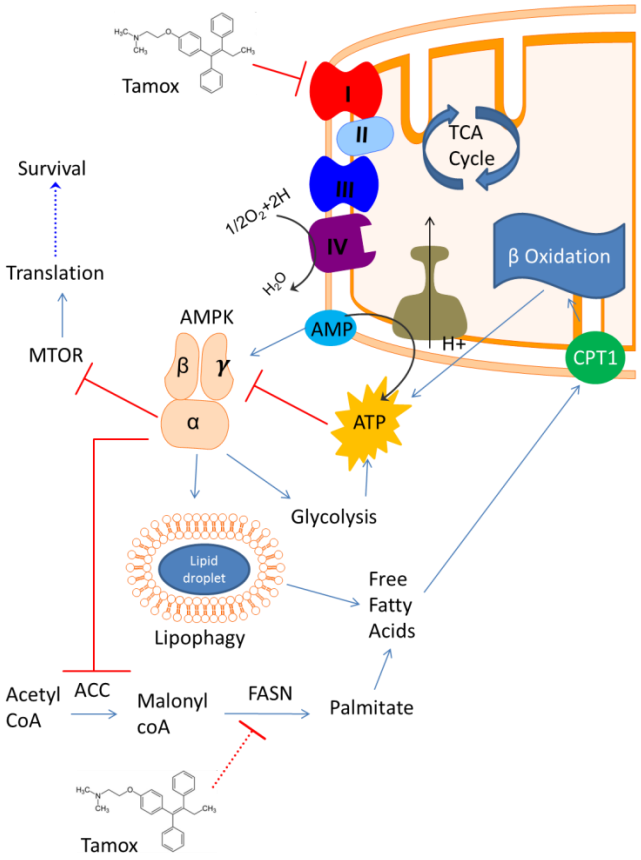

Previous page – **Figure IV-1: Model of the effects of Tamoxifen on metabolism.** Tamoxifen inhibits oxygen consumption at complex I of the mitochondrial electron transport chain. This increases the AMP/ATP ratio and activates AMPK. Downstream effects of AMPK activation on cell survival, translation and autophagy are mediated in an isoform specific manner. Tamoxifen treatment also increases cellular dependence on glycolysis and alters fatty acid metabolism.

Tamoxifen inhibition of Oxygen consumption

Chapter II describes a novel mechanism by which tamoxifen treatment inhibits cellular oxygen consumption. Tamoxifen acts directly on the mitochondria, upstream of complex II, independently of ER signaling. We see inhibition of oxygen consumption across a panel of multiple cancer cell lines, therefore these effects have the potential to expand the use of tamoxifen beyond ER+ BC. Through degradation of ERα by fulvestrant and knock out using CRISPR-cas9 we have demonstrated that ERα signaling does not contribute to the effects of tamoxifen on respiration. However, the impact of ERβ signaling on tamoxifen inhibition of oxygen consumption was beyond the scope if this work. ERβ and ERα have both overlapping and distinct biological functions. ERβ is expressed in breast tissue but has been reported to be downregulated in BC due to promotor methylation, suggesting it may function as a tumor suppressor. However immunohistochemical staining shows ERβ expression in approximately 2/3 of BC samples[81]. Tamoxifen functions as an ERβ antagonist[82] but the role of ERβ in response to therapy remains unclear. ERβ expression is correlated with improved survival[83] but has also been shown to be increased in tamoxifen resistant cases[84]. Important for elucidating the metabolic effects of tamoxifen is the reported expression of ERβ in mitochondria[85,86]. While we did not test whether ERβ signaling contributes to the ability of tamoxifen to alter respiration, it is unlikely. Inhibition of oxygen consumption occurs within 2 minutes of the addition of tamoxifen, indicating that these effects are likely not the result of transcriptional changes promoted by nuclear receptors. However,

more experiments would be needed to determine if ERβ contributes to the effects of tamoxifen on BC cell metabolism.

This study suggests that tamoxifen is an inhibitor of electron transport chain complex I. Complex I inhibitors have become of particular interest as cancer therapeutics due to the anti-cancer properties of metformin, a reported complex I inhibitor[42]. However, many complex I inhibitors such as rotenone are highly toxic. Our data demonstrates that tamoxifen inhibits oxygen consumption faster and at lower doses than metformin. The data reported in this study as well as numerous clinical trials demonstrating the safety of tamoxifen at a large range of dosages support the clinical use of tamoxifen as a safe and well tolerated complex I inhibitor. However, we cannot completely rule out other mitochondrial targets. Previous studies have reported tamoxifen to alter the mitochondrial membrane potential[23,65] and inhibit at complex III[87]. While our data does not support these mechanisms, future studies such as binding assays and crystallography would be necessary to determine the exact interaction site of tamoxifen with mitochondria.

The many phase I/II clinical trials that explored high dose tamoxifen as a single agent or in combination with cytotoxic chemotherapeutics demonstrated safety, but little clinical efficacy. Our *in vitro* data suggests that tamoxifen treatment may be effective in combination with other metabolically targeted agents, such as glycolytic inhibitors. Moreover, this study also suggests that tamoxifen may be effective in combination with oncogene targeted therapy. Future work would be necessary to demonstrate the efficacy of these combinations *in vivo.* It would also be worthwhile to investigate the ability of tamoxifen to function as a radiosensitizer. Tumor hypoxia significantly limits the success of radiotherapy for cancer treatment. The presence of intracellular oxygen enhances the effect of radiation induced DNA damage through the “oxygen effect”. Ionizing radiation

results in the generation of carbon centered radicals in DNA and proteins which can be repaired by hydrogen donors in the cell, a process known as chemical restitution. In the presence of oxygen, peroxidation of radicals occurs in a process known as damage fixation. These peroxy radicals cannot be repaired, resulting in increased DNA damage and cell death[88]. To date, strategies to reduce hypoxia for radiosensitization have not achieved regular clinical use. An agent that decreases tumor oxygen consumption has the potential to act as a radiosensitizer or enhancer because it would increase local pO_2 and reduce hypoxia[46]. Such compounds including metformin[89], nelfinavir[90], and PI3K/mTOR inhibitors[91] have been shown to reduce hypoxia and radiosensitize tumors. Atovoquone, an anti-malarial drug that targets mitochondrial electron transport complex III[92], is also in clinical trials as a radiosensitizer. In addition to reducing oxygen consumption, metformin has also been shown to act as a radiosensitizer through AMPK dependent mechanisms[93,94]. Based on this literature and the data described in this study, it would be reasonable to hypothesize that tamoxifen would reduce tumor hypoxia and function as a radiosensitizer. Additional experiments *in vitro* and *in vivo* are needed to test this.

Tamoxifen activation of AMPK

Chapter II describes tamoxifen as a novel activator of AMPK. Tamoxifen treatment results in an increase in the AMP/ATP ratio and phosphorylation of AMPKα. Activation of AMPK by tamoxifen further supports the hypothesis that tamoxifen acts as a complex I inhibitor as well as the use of tamoxifen as a metabolically targeted therapeutic. Multiple kinases have been reported to phosphorylate AMPK. In this study we explored the role of the two most prominent AMPK-Kinases, LKB1 and CaMKK2 in the mechanism by which tamoxifen activates AMPK. Using both genetic and

pharmacological means, we determined that both kinases play a role in AMPK activation following tamoxifen treatment and that their prominence is largely cell type dependent. CaMKK2 has been shown to phosphorylate AMPK in response to AICAR treatment in cells lacking LKB1[95]. However, CaMKK2 also activates AMPK in response to an increase in intracellular calcium concentrations[96]. Therefore, the role of CaMKK2 in activation of AMPK following tamoxifen treatments poses the question of whether calcium dysregulation by tamoxifen may also be involved. Tamoxifen has been previously shown to alter calcium signaling in BC and glioma cells[97]. In order to determine if this effect is involved in activation of AMPK, chelators such as BAPTA-AM could be used. AMPK is also allosterically activated by AMP binding, even without phosphorylation of the AMPKα[56], our data agrees with these reports as we see phosphorylation of ACC with tamoxifen treatment even without phosphorylation of AMPK.

The role of AMP allosteric activation of AMPK as well as the involvement of CaMKK2 in tamoxifen-mediated activation of AMPK is important to note because LKB1 is a tumor suppressor and is frequently lost in cancers. Recent studies have shown that phenformin is effective as a single agent in a mouse model of KRAS LKB1-/- NSCLC, suggesting that AMPK activators may be therapeutic in LKB1-/- cancers[98]. Thus our data suggests that tamoxifen treatment may also be effective in these cancers.

Chapter II describes the role of AMPK in BC cell survival of tamoxifen treatment to be mediated by isoform specific effects. We see protection from tamoxifen mediated cytotoxity in CrspAMPKα1 knock out cell, while loss of AMPKα2 results in increased cell death. In our system, both isoforms are needed to inhibit ACC, while inhibition of the mTOR pathway is AMPKα1 dependent, yet activation of autophagy can be promoted by either isoform. Upon loss of AMPKα1 we see increased AMPKα2 expression and it

remains unclear whether it is the loss of AMPKα1 or overexpression of AMPKα2 that rescues cells from tamoxifen. Moreover, it is still unclear which downstream targets are responsible for the survival effects of each isoform and more work would be needed to elucidate these specific mechanisms. While this work identifies potentially novel isoform specific roles for AMPKα in mediating downstream signaling effects, it is important to recognize that these differences may be both cell type dependent as well as stress dependent. More work would be needed to determine reproducibility across multiple contexts.

Tamoxifen alters glucose and fatty acid metabolism

Chapter III aims to characterize the metabolic changes that accompany tamoxifen inhibition of OXPHOS. It is well established that inhibition of respiration results in an upregulation of glycolytic activity and this effect is seen in tamoxifen treated BC cells as well. Using [$^{13}C_6$]-glucose labeling we see the contribution of glucose carbons to lactate, acetyl-CoA, and malonyl-CoA to be increased with tamoxifen treatment. However we do not see a significant change in labeled-glucose incorporation into the TCA cycle. Inhibition of OXPHOS is often correlated with a reduction in TCA cycle activity due to the buildup of NADH and $FADH_2$. This study did not examine total levels of TCA cycle intermediates, therefore it is possible that tamoxifen reduces overall TCA cycle activity, without any change in the percent labeling from glucose. It would be important to further examine the effects of tamoxifen on TCA cycle activity as many of the intermediates can be used for synthesis of other essential macromolecules such as amino acids and nucleotides[99,100]. Moreover, investigating whether there is any change in the NAD+/NADH and FAD/$FADH_2$ levels upon tamoxifen treatment would also be worthwhile. Further examination of TCA cycle activity, amino acids and nucleotide

synthesis pathways, as well as reducing equivalents upon tamoxifen treatment could potentially identify opportunities to increase tamoxifen response by targeting these altered pathways.

Chapter III also reports significant changes in fatty acid metabolism upon tamoxifen treatment. Acyl-CoA quantification showed an unexpected accumulation of long chain CoA species. Labeling experiments indicated that these were not synthesized *de novo* from glucose or glutamine and accumulation of malonyl-CoA suggests an inhibition of FASN. Loss of total neutral lipid content in the cell suggests the source of these free fatty acids to be break down of lipid droplets. However, we did see an increase in acetate label incorporation into the total lipid pool upon tamoxifen treatment. Yet this experiment did not identify what species of lipids were labeled with ^{14}C acetate, nor did it quantify the total levels of any species. As a result the interpretation of this data is quite limited. It suggests that BC cells treated with tamoxifen shift the fatty acid carbon source from glucose or glutamine to acetate, which is in agreement with previous reports of cells under metabolic stress[77]. Further investigation into cellular acetate metabolism with LC-MS/MS analysis of ^{13}C acetate labeling into the acyl-CoAs would provide additional clarity. Moreover, if acetate utilization is required in tamoxifen treated cells, ACSS2, the enzyme that converts acetate to acetyl-CoA may be a good target to increase tamoxifen efficacy.

Supplementation of BC cells with oleic acid completely rescues cells from tamoxifen treatment and restores mTOR activity. It is easy to hypothesize that these effects are due to β-oxidation generation of ATP and macromolecular intermediates. However, elevated malonyl-CoA levels seen with tamoxifen treatment suggest that the CPT-1 transporter is inhibited. Therefore β-oxidation would be blocked under these conditions. LC-MS/MS analysis of ^{13}C labeled oleate incorporation into short chain Acyl-

CoA's would provide insight into whether oleic acid undergoes β-oxidation. Another possible explanation for the pro-survival effects of oleic acid on tamoxifen treated cells could be the use of oleic acid to repair damaged membranes. Tamoxifen has been shown to accumulate in, and alter the properties of cellular membranes[101,102]. More experiments would be needed to assess the extent to which intracellular membranes are compromised by tamoxifen treatment and if oleic acid plays any role in repair.

Therapeutic opportunities exploiting the metabolic effects of tamoxifen

Metabolic flexibility allows for the upregulation of pathways to compensate for a physiological or pharmacological blockade. This plays a role in ability of cancer cells to survive nutrient deprivation characteristic of the tumor microenvironment as well as limited the use of metabolically targeted agents. It has been postulated that dual targeting of these compensatory pathways would improve the efficacy of metabolically targeted therapeutics

Our data suggest that combination treatment with tamoxifen and glycolysis inhibitors may be clinically effective, however in an *in vivo* mouse model of triple negative BC, we did not see any effect on tumor growth with tamoxifen and the glycolytic inhibitor 3BP. The lack of efficacy *in vivo* may be due to multiple factors including the resistance of slowly proliferating tumors to metabolic stress, delivery of tamoxifen in a lipid vehicle, and dose limiting toxicity of 3BP. Additional studies are warranted to determine if this combination treatment could be effective in reducing tumor growth in other models. The development of improved glycolytic inhibitors is also greatly needed. No available glycolytic inhibitors have reached regular clinical use despite being extensively studied. Limitations to the development of such compounds include the

ubiquitous expression of glycolytic enzymes in all tissues and the dependence of sensitive organs such as the brain on glucose metabolism[31,103].

Chapter III also describes the success of tamoxifen as a treatment in OXPHOS addicted tumor cell populations. Inhibition of oncogenes that promote the Warburg effect by targeted therapies result in increased respiration in resistant populations. These resistant populations result in therapeutic failure and disease progression in patients. Using a model of BRAF-inhibitor resistant melanoma, treatment with tamoxifen can reduce oxygen consumption preferentially kill the resistant cells. We hypothesize that the increased cell death is due to the inability of these cells to respire in the presence of tamoxifen and the ensuing metabolic stress. However we have not determined the exact mechanism by which tamoxifen results in cytotoxicity in this population. More experiments would be necessary to determine if loss of ATP and activation of AMPK, loss of reducing equivalents and an increase in ROS, as well as inability of these cells to synthesize macromolecular intermediates contributes to cell death. In addition, Investigating whether this effect occurs *in vivo* would be necessary to determine whether the addition of tamoxifen treatment to BRAF-inhibitors improves survival and reduces recurrence in melanoma.

CHAPTER 5: Materials and Methods

Chemicals and antibodies. Tamoxifen, fulvestrant, methyl succinate, STO609, oleic acid-BSA were purchased from Sigma Aldrich. The following rabbit polyclonal Antibodies were obtained from Cell Signaling: AMPKα, AMPKα1, phos-AMPKα, LKB1, phos-ACC, ACC, Phos-p70s6K, phos-s6, phos-4EBP1, cleaved PARP, cleaved caspase 3, and LC3B. ERα antibody purchased from Genetex. AMPKα2 antibody purchased from Millipore. siRNA against PRKAA2, LKB1 and CaMKK2 was purchased from Dharmacon.

Cell culture. Cell lines were cultured in Dulbecco's modified eagles medium (DMEM) supplemented with 10% FBS, 1% penicillin/streptomycin, and HEPES at 37°C humidified 5% CO_2 atmosphere. MCF7, MDA-MB-231 and 4175 cell lines were a gift from Andy Minn. LCC1 cells were a gift from Robert Clarke. WM9 and 1205Lu cells were a gift from Meenhard Herlyn (Wistar Institute). Cell lines were authenticated through genetic testing by ATCC.

Oxygen consumption measurements. Oxygen consumption was measured using a YSI 5300a Biological oxygen monitor. Electrodes were equilibrated in media for 10 minutes. Cells were trypsinized and suspended at $2x10^7$cells per mL and injected into the chamber at a 1:10 dilution. After oxygen consumption rate was recorded, drug was injected into the chambers at 10 µM increments, allowing consumption rate to be determined after each injection. Total protein per chamber was quantified by Lowry assay.

Isolation of liver mitochondria. The liver was removed from a sacrificed mouse and homogenized in 8 volumes of sucrose buffer (0.25 M sucrose, 0.02 M KCl, 0.005 M $MgCl_2$, 0.01 M KH_2PO_4 (pH= 7.4). The homogenate was spun at 600 x g for 5 min at

4°C. The supernatant was then transferred to a new tube and centrifugation was repeated. Cleared supernatant was spun at 9000 x g for 10 min at 0°C and the pellet was resuspended in sucrose buffer. The following conditions were used for respiration measurements: Complex 1 respiration: Sucrose buffer + 0.1 mM ADP, 5 mM glutamate and 5 mM malate. Complex 2 respiration: Sucrose buffer + 0.1 mM ADP and 5 mM sodium succinate.

Respiration of permeabilized cells. BC cells were trypsinized and washed once with sucrose buffer. Cells were diluted to $2x10^6$ cells per mL in sucrose buffer and digitonin was added at 25ug/mL and incubated at room temperature for 2 minutes, Permeabilization was confirmed with trypan blue stain. Oxygen consumption measurements were performed as described for liver mitochondria.

Cell survival assays. Modified MTT assay: Cells were plated in a 24 well plate at $5x10^4$ cells per well and allowed to attach overnight. After drug incubation, cells were washed, re-fed with fresh media and grown for 5-7 days until control cells reached confluency. An MTT assay kit (Roche) was used to measure survival and proliferation following the manufacturer's instructions. Clonogenic survival assay: Cells were plated at 80% confluency in 60mm dishes and allowed to adhere overnight. Cells were treated with experimental conditions, trypsinized, washed, re-plated at low density (100-1000 cells) and incubated until visible colonies grew from single cells. Colonies stained with crystal violet and counted. Survival was reported as fraction of colony count over number of cells plated, normalized to control conditions.

I**mmunoblot analysis**. Cells were lysed using nonident p-40 buffer (1% NP-40, 1 mM phenylmethylsulfonyl fluoride, 1X Complete Mini protease inhibitor cocktail [Roche], 1X phosphatase inhibitor cocktail 2 [Sigma] in PBS.) Protein concentrations of lysates were determined using DC protein assay (BioRad). Equal amounts of protein were resolved on sodium dodecyl sulfate polyacrylamide gels and transferred to polyvinylidene fluoride membranes. Membranes were blocked with 5% non-fat dried milk in TBS-T (20 mM Tris, 137 mM NaCl, 0.1% Tween-20; pH 7.6) and then incubated in primary antibody followed by secondary antibody. Proteins were visualized by incubating membranes in ECL chemicals and exposing to film.

Generation of CRISPR-Cas9 knockout cell lines. Knock out cell lines were generated using the CRISPR-cas9 system as previously described[104]. sgRNAs were designed to target the first exon of the genes of interest using the CRISPR design tool at http://crispr.mit.edu/. Two sgRNA sequences were chosen for each gene of interest (See table below). Briefly, sgRNA's were cloned into CRISPR-cas9 plasmid. pSpCas9(BB)-2A-Puro (PX459) was a gift from Feng Zhang (Addgene plasmid # 48139) . Cells were transfected using lipofectamine 2000 and carrier DNA. Media was changed 24hrs after transfection and cells were selected with puromycin for 48 hrs. Remaining cells grown up and clones were selected. Clones were screened for gene excision or mutation by DNA gel and expression of the protein of interested by western blot. Knock out was successful using both *PRKAA1* sgRNAs 1 and 2. Knock out of *ESR1* expression required combined transfection of sgRNA 1 and 2.

sgRNA	Sequence
PRKAA1 1F	CACCGTACATTCTGGGTGACACGCT
PRKAA1 1R	AAACAGCGTGTCACCCAGAATGTAC
PRKAA1 2F	CACCGATTCGGAGCCTTGATGTGGT
PRKAA1 2R	AAACACCACATCAAGGCTCCGAATC
ESR1 1F	CACCGACCGTAGACCTGCGCGTTGG
ESR1 1R	AAACCCAACGCGCAGGTCTACGGTC
ESR1 2F	CACCGCTCGCGCACCGTGTAGCCGC
ESR1 2R	AAACGCGGCTACACGGTGCGCGAGC

Table V-1: sequences of sgRNA for CRISPR-cas9 knock out cell lines

HPLC quantification of AMP and ATP. AMP and ATP quantified using a previously published method [105]. Briefly, 2-4x10^6 cells were plated in 10cm^2 dishes and treated with tamoxifen. Cells were then pelleted and nucleotides extracted with perchloric acid. Extracts were analyzed by ion pair reverse phase HPLC. Analysis was carried out on a Jasco HPLC. Separation was performed on SUPELCOSIL C18 column (15 cm x 4.6 mm, 3 µm particle size) in combination with a Supelguard Acentis C18 guard column (2 cm x 4.0 mm) from Sigma.

LC-MS/MS metabolite analysis. Liquid chromatography-selected reaction monitoring (LC-SRM)/MS was used for analysis of acyl-CoA thioesters. Methods were previously described in detail[106]. CoAs were separated using a reversed-phase HPLC Phenomenex Luna C18 column (2.0 mm × 150 mm, particle size 3.5 µm) with 5 mM ammonium acetate in water as solvent A, 5 mM ammonium acetate in ACN/water (95:5; v/v) as solvent B, and ACN/water/formic acid (80:20:0.1; v/v/v) as solvent C. Samples were analyzed using an API 4000 triple-quadrupole mass spectrometer (Applied Biosystems, Foster City, CA) in the positive electrospray (ESI) mode. Samples (10 µL)

were injected using a Leap CTC autosampler (CTC Analytics, Switzerland) where they were maintained at 4 °C.

Short-chain and Long-chain acyl-CoA extraction. *Short-chain acyl-CoA extraction***.** Extractions were performed as described in detail previously[106]. Briefly, cells were lifted manually with a cell scraper, centrifuged at 500 x g for 5 min and resuspended in 1 mL of ice-cold 10% TCA and pulse-sonicated for 30 s on ice using a sonic dismembranator (Fisher), followed by a 5 min centrifugation at 15,000 x g. The supernatant was transferred to a fresh tube, and the pellet was discarded. The supernatant was purified by solid-phase extraction as follows: Oasis HLB 1 cm^3 (30 mg) SPE columns (Waters) were conditioned with 1 mL of methanol followed by 1 mL of water. The collected supernatant was applied, washed with 1 mL of water, and finally eluted using three subsequent applications of 0.5 mL of methanol containing 25 mM ammonium acetate. Eluted compounds were dried down under nitrogen and resuspended in 100 µL of 5% 5-SSA. For isotopologue analysis, the same extraction was used, except that no internal standard was added. *Long-chain acyl-CoAs extraction*- Extractions were performed as described in detail previously[107]**.** Cells were lifted manually with a cell scraper, centrifuged at 500 x g for 5 min and resuspended in 550 µL/10 cm^2 plate of ACN:IPA (3:1; v/v). The internal standard prepared using stable isotope labeling by essential nutrients in cell culture (SILEC) was added (200 µL) and samples were pulse sonicated with a probe tip sonicator on ice 30 times for 0.5 s. 250 µL of 100 mM KH_2PO_4 (pH 6.7) was added to the samples, then vortex-mixed and spun down for 10 min at 16,000 x g at 4°C. The supernatant was transferred to a glass tube and acidified with 125 µL of glacial acetic acid. SPE columns were equilibrated with 1 mL of ACN/IPA/water/acetic acid (9:3:4:4; v/v/v/v) washing solvent. Samples were transferred to the columns, which

were washed two times with 1 mL of the washing solvent. The acyl-CoAs were then eluted by washing the columns twice with 500 µL methanol/250 mM ammonium formate (4:1; v/v) into glass tubes. After evaporation to dryness under nitrogen gas, the eluates were re-dissolved in 50 µL of water/ACN (7:3; v/v) containing 5 % SSA (w/v) and transferred to HPLC vials for LC-SRM/MS analysis.

Lactate extraction and analysis by LC-MS/MS: Media was aspirated and cells were quenched by the direct addition of 1 mL -80 °C 4:1 methanol:water (v/v) to the cell culture dish. Plates were placed at -80 °C for 20 min then scraped and transferred into Eppendorf tubes. Samples were pulse sonicated on ice for 30 sec at a rate of 1 pulse/sec prior to centrifugation at 16,000 x *g* at 4 ^{o}C for 10 min. The supernatants were then transferred to clean glass tubes and evaporated to dryness under nitrogen. Dried residues were resuspended in 100 µL of mobile phase A for LC-MS analysis. For labeling studies cells were grown in media omitting glucose supplemented with 1 mg/mL [$^{13}C_6$]-glucose. Details of the LC-MS/MS analysis have been describes in detail previously [108].

Quantification of tamoxifen and metabolites in tumor tissue. Tumor was removed from mouse under anesthesia and flash frozen in liquid N_2. Frozen tissue was weighed and homogenized by electric homogenizer on ice in 4:1 methanol:water (v/v). Samples were then centrifuged at 16,000 x *g* at 4 ^{o}C for 10 min. 10 µL of the resulting supernatant was analyzed by reverse phase LC-MS/MS utilizing teniposide as the internal standard for absolute quantification.

siRNA transfection. Cells were grown in 60 mm dishes to approximately 60% confluency. The cells were transfected with lipofectamine RNAi Max and siRNA to *PRKAA2* at 50 nM mixed in OptiMEM. Transfection mixture was added to the cell culture plates in complete DMEM and incubated for 24 hrs before the plates were washed and refed with fresh complete DMEM. Cells were cultured for an additional 48 hrs before treatment with tamoxifen.

BODIPY 493/503 staining. BODIPY 493/503 was purchased from Molecular Probes. Staining solution was made up at 2 µg/mL in PBS. After drug treatments, cells were fixed using 4% paraformaldehyde and stored at 4°C. Neutral lipid staining was performed by pelleting the cells and re-suspending in staining solution and incubated for 10 mins at room temperature. Cells were washed 2x with PBS, suspended in 500 µL PBS and strained. Cells were analyzed for mean BODIPY stain intensity by flow cytometry (FL1-H).

[^{14}C] acetate labeling of lipid pools: The protocol has been previously described[109]. Briefly, tamoxifen or vehicle treated ells were incubated with [^{14}C]acetate for 2 hours. The cells were then washed with PBS/EDTA and trypsinized. Pellets were washed twice with PBS, and fatty acids were extracted with chloroform-methanol (1:1) for 30 min. The extract was dried under N_2 and then extracted with water-saturated butanol. Butanol was evaporated under N_2, and labeled fatty acids were detected by scintillation counting

[^{35}S] labeling. Cells were plated in 60 mm dish and treated for experimental conditions. Cells were incubated with methionine/cysteine free media for 30 min. Hot labeling media

was made up at 0.075 mCi/mL [^{35}S]-methionine/cysteine. Cells were incubated with labeling media for 30 mins. Cells were washed with cold PBS and harvested for protein. Protein assay performed on cold samples and equal amounts of [^{35}S] labeled protein were resolved on sodium dodecyl sulfate polyacrylamide gels. Gel was washed with fixing solution (water with 20% methanol, 10% acetic acid) for 30 min, washed with DI water, then washed with enlightening solution (PerkinElmer) for 30 min. Gel was dried overnight using a BioRad gel drying apparatus. The gel was exposed to autoradiography film at -80°C and film was developed.

Orthotopic xenograft tumors: Four-week old female nu/nu mice were purchased from Charles River Laboratories and housed in the University of Pennsylvania animal facility maintained on a 12 h light/dark cycle and given free access to water and food *ad libitum*. 2x10^{6} 4175 cells suspended in 50 µL of a 50/50 mixture of PBS and Matrigel Matrix basement membrane (Corning) were injected into the mammary fat pad. Tumor growth was measured twice weekly by calipers. Tumor volume was calculated by the modified ellipsoid formula: Tumor volume= 1/2(length × width^{2})[110]. All animal experiments were performed in accordance with the “Guide for the Care and Use of Laboratory Animals” of the National Research Council of the National Academies and approved by the University of Pennsylvania Institutional Animal Care and Use Committee.

***In vivo* Tamoxifen and 3BP treatment**. Tamoxifen was dissolved 20 mg in 200 µL ethanol and 800 µL peanut oil. Ethanol was evaporated off overnight. 3BP was dissolved at 0.5 mg/mL in sterile PBS immediately before injection. Mice were dosed via intraperitoneal injection.

Protein analysis from tumors. Tumors were removed under isoflurane anesthesia and the animals immediately sacrificed. Tumors were flash frozen in liquid N_2. Lysis buffer was 50 mM HEPES pH 7.4, 150 mM NaCl, 1.5 mM $MgCl_2$, 1 mM EGTA. Immediately before use PMSF, complete mini, and phosphatase inhibitor cocktail was added. On dry ice, the tumor was cut and random pieces from different sections of the tumor were weighed and added to lysis buffer at 40mg/mL. The tumor was homogenized by electric homogenizer on ice. 1% Triton-X was then added and the lysate sonicated. Samples were then set on ice for 10 minutes then spun at 12000 rpm and 4°C for 10 min and the pellet discarded.

Statistical analysis: All statistical analyses were performed using a two-tailed Student's t test assuming homoscedasticity. A p value < 0.05 was considered statistically significant.

REFERENCES

1. Kamangar, F., Dores, G. M. & Anderson, W. F. Patterns of cancer incidence, mortality, and prevalence across five continents: defining priorities to reduce cancer disparities in different geographic regions of the world. *J. Clin. Oncol.* **24,** 2137–50 (2006).

2. Weigelt, B., Peterse, J. L. & van 't Veer, L. J. Breast cancer metastasis: markers and models. *Nat. Rev. Cancer* **5,** 591–602 (2005).

3. Dai, X. *et al.* Breast cancer intrinsic subtype classification, clinical use and future trends. *Am. J. Cancer Res.* **5,** 2929–2943 (2015).

4. Ali, S., Buluwela, L. & Coombes, R. C. Antiestrogens and their therapeutic applications in breast cancer and other diseases. *Annu. Rev. Med.* **62,** 217–32 (2011).

5. Musgrove, E. a & Sutherland, R. L. Biological determinants of endocrine resistance in breast cancer. *Nat. Rev. Cancer* **9,** 631–43 (2009).

6. Osborne, C. K. Tamoxifen in the treatment of breast cancer. *N. Engl. J. Med.* **339,** 1609–1618 (1998).

7. Matsuoka, H. *et al.* Tamoxifen inhibits tumor cell invasion and metastasis in mouse melanoma through suppression of PKC/MEK/ERK and PKC/PI3K/Akt pathways. *Exp. Cell Res.* **315,** 2022–2032 (2009).

8. Gundimeda, U., Chen, Z. H. & Gopalakrishna, R. Tamoxifen modulates protein kinase C via oxidative stress in estrogen receptor-negative breast cancer cells. *J. Biol. Chem.* **271,** 13504–13514 (1996).

9. O, Brian, C. A., Liskamp, R. M., Solomon, D. H. & Weinstein, I. B. Inhibition of protein kinase C by tamoxifen. *Cancer Res.* **45,** 2462–2465 (1985).

10. McClay, E. F., Albright, K. D., Jones, J. a, Christen, R. D. & Howell, S. B. Tamoxifen modulation of cisplatin sensitivity in human malignant melanoma cells. *Cancer Res.* **53,** 1571–1576 (1993).

11. Tavassoli, M. *et al.* Tamoxifen inhibits the growth of head and neck cancer cells and sensitizes these cells to cisplatin induced-apoptosis: role of TGF-beta1. *Carcinogenesis* **23,** 1569–1575 (2002).

12. Stuart, N. S. *et al.* High-dose tamoxifen as an enhancer of etoposide cytotoxicity. Clinical effects and in vitro assessment in p-glycoprotein expressing cell lines. *Br. J. Cancer* **66,** 833–839 (1992).

13. Brandes, B. A. A. *et al.* Procarbazine and high-dose tamoxifen as a second-line regimen in recueent high-grade gliomas: A phae II study. *J. Clin. Oncol.* **17,** 645–650 (1999).

14. Couldwell, W. T. *et al.* Treatment of recurrent malignant gliomas with chronic oral high-dose tamoxifen. *Clin. Cancer Res.* **2,** 619–622 (1996).

15. Pollack, I. F. *et al.* A phase I study of high-dose tamoxifen for the treatment of refractory malignant gliomas of childhood. *Clin. Cancer Res.* **3,** 1109–1115 (1997).

16. Tang, P. a. *et al.* A phase II study of carboplatin and chronic high-dose tamoxifen in

patients with recurrent malignant glioma. *J. Neurooncol.* **78,** 311–316 (2006).

17. McClay, E. F. *et al.* A phase I and pharmacokinetic study of high dose tamoxifen and weekly cisplatin in patients with metastatic melanoma. *Cancer* **79,** 1037–1043 (1997).

18. Creagan, E. T., Ingle, J. N., Ahmann, D. L. & Green, S. J. Phase II stusy of high-dose tamoxifen (NSC-180973) in patients with disseminated Malignant melanoma. *Cancer* **49,** 1353–1354 (1982).

19. Perez, E. a *et al.* Phase I trial of high-dose tamoxifen in combination with cisplatin in patients with lung cancer and other advanced malignancies. *Cancer Invest.* **21,** 1–6 (2003).

20. Bergan, R. C. *et al.* A Phase II study of high-dose tamoxifen in patients with hormone-refractory prostate cancer. *Clin. cancer Res.* **5,** 2366–2373 (1999).

21. Lien, E. a, Solheim, E. & Ueland, P. M. Distribution of tamoxifen and its metabolites in rat and human tissues during steady-state treatment. *Cancer Res.* **51,** 4837–4844 (1991).

22. Moreira, P. I., Custódio, J., Moreno, A., Oliveira, C. R. & Santos, M. S. Tamoxifen and estradiol interact with the flavin mononucleotide site of complex I leading to mitochondrial failure. *J. Biol. Chem.* **281,** 10143–52 (2006).

23. Cardoso, C. M. P., Moreno, A. J. M., Almeida, L. M. & Custódio, J. B. a. 4-Hydroxytamoxifen induces slight uncoupling of mitochondrial oxidative phosphorylation system in relation to the deleterious effects of tamoxifen. *Toxicology* **179,** 221–32 (2002).

24. Vander Heiden, M. G., Cantley, L. C. & Thompson, C. B. Understanding the Warburg effect: the metabolic requirements of cell proliferation. *Science (80-.).* **324,** 1029–1033 (2009).

25. Koppenol, W. H., Bounds, P. L. & Dang, C. V. Otto Warburg's contributions to current concepts of cancer metabolism. *Nat. Rev. Cancer* **11,** 325–337 (2011).

26. DeBerardinis, R. J., Lum, J. J., Hatzivassiliou, G. & Thompson, C. B. The Biology of Cancer: Metabolic Reprogramming Fuels Cell Growth and Proliferation. *Cell Metab.* **7,** 11–20 (2008).

27. Boroughs, L. K. & DeBerardinis, R. J. Metabolic pathways promoting cancer cell survival and growth. *Nat. Cell Biol.* **17,** 351–359 (2015).

28. Thompson, C. B. Metabolic enzymes as oncogenes or tumor suppressors. *N. Engl. J. Med.* **360,** 813–815 (2009).

29. Jones, R. G. & Thompson, C. B. Tumor suppressors and cell metabolism : a recipe for cancer growth Tumor suppressors and cell metabolism : a recipe for cancer growth. 537–548 (2009). doi:10.1101/gad.1756509

30. Bobrovnikova-Marjon, E. & Hurov, J. B. Targeting Metabolic Changes in Cancer: Novel Therapeutic Approaches. *Annu. Rev. Med.* **65,** 157–170 (2014).

31. Ganapathy-Kanniappan, S. & Geschwind, J.-F. H. Tumor glycolysis as a target for cancer therapy: progress and prospects. *Mol. Cancer* **12,** 152 (2013).

32. Vander Heiden, M. G. Targeting cancer metabolism: a therapeutic window opens. *Nat. Rev. Drug Discov.* **10,** 671–684 (2011).

33. Hu, H. *et al.* Phosphoinositide 3-Kinase Regulates Glycolysis through Mobilization of Aldolase from the Actin Cytoskeleton. *Cell* **164,** 433–446 (2016).

34. Cerniglia, G. J. *et al.* The PI3K/Akt Pathway Regulates Oxygen Metabolism via Pyruvate Dehydrogenase (PDH)-E1α Phosphorylation. *Mol. Cancer Ther.* **14,** 1928–1939 (2015).

35. Solaini, G., Sgarbi, G. & Baracca, A. Oxidative phosphorylation in cancer cells. *Biochim. Biophys. Acta* **1807,** 534–542 (2011).

36. Ward, P. S. & Thompson, C. B. Metabolic Reprogramming: A Cancer Hallmark Even Warburg Did Not Anticipate. *Cancer Cell* **21,** 297–308 (2012).

37. Viale, A., Corti, D. & Draetta, G. F. Tumors and mitochondrial respiration: a neglected connection. *Cancer Res.* **75,** 3685–3686 (2015).

38. Viale, A. *et al.* Oncogene ablation-resistant pancreatic cancer cells depend on mitochondrial function. *Nature* **514,** 628–632 (2014).

39. LeBleu, V. S. *et al.* PGC-1α mediates mitochondrial biogenesis and oxidative phosphorylation in cancer cells to promote metastasis. *Nat. Cell Biol.* **16,** 992–1003 (2014).

40. Yuan, P. *et al.* Phenformin enhances the therapeutic benefit of BRAF V600E inhibition in melanoma. *PNAS* **110,** 18226–18231 (2013).

41. Lagadinou, E. D. *et al.* BCL-2 inhibition targets oxidative phosphorylation and selectively eradicates quiescent human leukemia stem cells. *Cell Stem Cell* **12,** 329–341 (2013).

42. Wheaton, W. W. *et al.* Metformin inhibits mitochondrial complex I of cancer cells to reduce tumorigenesis. *Elife* **2014,** 1–18 (2014).

43. Haq, R. *et al.* Oncogenic BRAF regulates oxidative metabolism via PGC1α and MITF. *Cancer Cell* **23,** 302–315 (2013).

44. Ying, H. *et al.* Oncogenic kras maintains pancreatic tumors through regulation of anabolic glucose metabolism. *Cell* **149,** 656–670 (2012).

45. Pollak, M. Targeting oxidative phosphorylation: Why, When, and How. *Cancer Cell* **23,** 263–264 (2013).

46. Lin, A. & Maity, A. Molecular pathways: A novel approach to targeting hypoxia and improving radiotherapy efficacy via reduction in oxygen demand. *Clin. cancer Res.* **21,** 1995–2000 (2015).

47. Mihaylova, M. M. & Shaw, R. J. The AMPK signalling pathway coordinates cell growth, autophagy and metabolism. *Nat. Cell Biol.* **13,** 1016–1023 (2011).

48. Steinberg, G. R. & Kemp, B. E. AMPK in Health and Disease. *Physiol. Rev.* **89,** 1025–1078 (2009).

49. Liang, J. & Mills, G. B. AMPK: A contextual oncogene or tumor suppressor? *Cancer Res.* **73,** 2929–2935 (2013).

50. Hardie, D. G., Ross, F. a. & Hawley, S. a. AMPK: a nutrient and energy sensor that maintains energy homeostasis. *Nat. Rev. Mol. Cell Biol.* **13,** 251–262 (2012).

51. Hardie, D. G. & Alessi, D. R. LKB1 and AMPK and the cancer-metabolism link - ten years after. *BMC Biol.* **11,** 36 (2013).

52. Faubert, B. *et al.* AMPK is a negative regulator of the warburg effect and suppresses tumor growth in vivo. *Cell Metab.* **17,** 113–124 (2013).

53. Zhou, J. *et al.* Inactivation of AMPK alters gene expression and promotes growth of prostate cancer cells. *Oncogene* **28,** 1993–2002 (2009).

54. Osborne, C. K., Wakeling, A. & Nicholson, R. I. Fulvestrant: an oestrogen receptor antagonist with a novel mechanism of action. *Br. J. Cancer* **90,** S2–S6 (2004).

55. Brünner, N. *et al.* Acquisition of hormone-independent growth in MCF-7 cells is accompanied by increased expression of estrogen-regulated genes but without detectable DNA amplifications. *Cancer Res.* **53,** 283–290 (1993).

56. Gowans, G. J., Hawley, S. a., Ross, F. a. & Hardie, D. G. AMP is a true physiological regulator of amp-activated protein kinase by both allosteric activation and enhancing net phosphorylation. *Cell Metab.* **18,** 556–566 (2013).

57. Minn, A. J. *et al.* Genes that mediate breast cancer metastasis to lung. *Nature* **436,** 518–524 (2005).

58. Zakikhani, M., Dowling, R., Fantus, I. G., Sonenberg, N. & Pollak, M. Metformin is an AMP kinase-dependent growth inhibitor for breast cancer cells. *Cancer Res.* **66,** 10269–73 (2006).

59. Engelholm, L. H. *et al.* AMPK: Lessons from transgenic knockout animals. *Front. Biosci.* 2103–2114 (2009).

60. Viollet, B. *et al.* The AMP-activated protein kinase αlpha2 catalytic subunit controls whole-body insulin sensitivity. *J. Clin. Invest.* **111,** 91–98 (2003).

61. Salt, I. *et al.* AMP-activated protein kinase: greater AMP dependence, and preferential nuclear localization, of complexes containing the alpha2 isoform. *Biochem. J.* **334,** 177–187 (1998).

62. Fox, M. M., Phoenix, K. N., Kopsiaftis, S. G. & Claffey, K. P. AMP-activated protein kinase α 2 isoform suppression in primary breast cancer alters AMPK growth control and apoptotic signaling. *Genes Cancer* **4,** 3–14 (2013).

63. Bursch, W. *et al.* Active cell death induced by the anti-estrogens tamoxifen and ICI 164 384 in human mammary carcinoma cells (MCF-7) in culture: the role of autophagy. *Carcinogenesis* **17,** 1595–1607 (1996).

64. Samaddar, J. S. *et al.* A role for macroautophagy in protection against 4-hydroxytamoxifen-induced cell death and the development of antiestrogen resistance. *Mol. Cancer Ther.* **7,** 2977–2987 (2008).

65. Cardoso, C. M., Custódio, J. B., Almeida, L. M. & Moreno, a J. Mechanisms of the deleterious effects of tamoxifen on mitochondrial respiration rate and phosphorylation efficiency. *Toxicol. Appl. Pharmacol.* **176,** 145–52 (2001).

66. Tuquet, C., Dupont, J., Mesneau, A. & Roussaux, J. Effects of tamoxifen on the electron transport chain of isolated rat liver mitochondria. *Cell Bio. Toxicol.* **16,** 207–219 (2000).

67. Biersack, H.-J., Bender, H. & Palmedo, H. FDG-PET in monitoring therapy of breast cancer. *Eur. J. Nucl. Med. Mol. Imaging* **31,** S112–7 (2004).

68. Dehdashti, F. *et al.* Positron emission tomographic assessment of ' metabolic flare ' to predict response of metastatic breast cancer to antiestrogen therapy. *Eur. J. Nucl. Med. Mol. Imaging* **26,** (1999).

69. Mortazavi-Jehanno, N. *et al.* Assessment of response to endocrine therapy using FDG PET/CT in metastatic breast cancer: a pilot study. *Eur. J. Nucl. Med. Mol. Imaging* **39,** 450–60 (2012).

70. Saphner, T., Triest-Robertson, S., Li, H. & Holzman, P. The association of nonalcoholic steatohepatitis and tamoxifen in patients with breast cancer. *Cancer* **115,** 3189–3195 (2009).

71. Wu, N. *et al.* AMPK-dependent degradation of TXNIP upon energy stress leads to enhanced glucose uptake via GLUT1. *Mol. Cell* **49,** 1167–1175 (2013).

72. Dörr, J. R. *et al.* Synthetic lethal metabolic targeting of cellular senescence in cancer therapy. *Nature* **501,** 421–5 (2013).

73. Sonveaux, P. *et al.* Targeting lactate-fueled respiration selectively kills hypoxic tumor cells in mice. *J. Clin. Invest.* **118,** 3930–3942 (2008).

74. Haq, R., Fisher, D. E. & Widlund, H. R. Molecular pathways: BRAF induces bioenergetic adaptation by attenuating oxidative phosphorylation. *Clin. Cancer Res.* **20,** 2257–2263 (2014).

75. Rambold, A. S., Cohen, S. & Lippincott-Schwartz, J. Fatty acid trafficking in starved cells: Regulation by lipid droplet lipolysis, autophagy, and mitochondrial fusion dynamics. *Dev. Cell* **32,** 1–15 (2015).

76. Worth, a. J., Basu, S. S., Snyder, N. W., Mesaros, C. & Blair, I. a. Inhibition of neuronal cell mitochondrial complex I with rotenone increases lipid -oxidation supporting acetyl-coenzyme A levels. *J. Biol. Chem.* **289,** 26895–26903 (2014).

77. Schug, Z. T. *et al.* Acetyl-CoA synthetase 2 promotes acetate utilization and maintains cancer cell growth under metabolic stress. *Cancer Cell* **27,** 57–71 (2015).

78. Ko, Y. H. *et al.* Advanced cancers: Eradication in all cases using 3-bromopyruvate therapy to deplete ATP. *Biochem. Biophys. Res. Commun.* **324,** 269–275 (2004).

79. Blackwell, K. L., Haroon, Z. A., Shan, S., Saito, W. & Broadwater, G. Tamoxifen Inhibits Angiogenesis in Estrogen Receptor-negative Animal Models Tamoxifen Inhibits Angiogenesis in Estrogen Receptor-negative Animal Models 1. **6,** 4359–4364 (2000).

80. López, M. *et al.* Tamoxifen-induced anorexia is associated with fatty acid synthase inhibition in the ventromedial nucleus of the hypothalamus and accumulation of malonyl-CoA. *Diabetes* **55,** 1327–1336 (2006).

81. Zhao, C., Dahlman-Wright, K. & Gustafsson, J.-Å. Estrogen receptor beta: an overview and update. *Nucl. Recept. Signal.* **6,** e003 (2008).

82. Barkhem, T. *et al.* Differential response of estrogen receptor alpha and estrogen receptor beta to partial estrogen agonists/antagonists. *Mol. Pharmacol.* **54,** 105–112 (1998).

83. Honma, N. *et al.* Clinical importance of estrogen receptor-beta evaluation in breast cancer patients treated with adjuvant tamoxifen therapy. *J Clin Oncol* **26,** 3727–3734 (2008).

84. Speirs, V., Malone, C., Walton, D. S., Kerin, M. J. & Atkin, S. L. Increased expression of estrogen receptor beta mRNA in tamoxifen-resistant breast cancer patients. *Cancer Res* **59,** 5421–5424 (1999).

85. Yang, S.-H. *et al.* Mitochondrial localization of estrogen receptor beta. *Proc. Natl. Acad. Sci. U. S. A.* **101,** 4130–5 (2004).

86. Pedram, A., Razandi, M., Wallace, D. C. & Levin, E. R. Functional Estrogen Receptors in the Mitochondria of Breast Cancer Cells. *Mol. Biol. Cell* **17,** 2125–2137 (2006).

87. Theodossiou, T. A., Yannakopoulou, K., Aggelidou, C. & Hothersall, J. S. Tamoxifen subcellular localization; Observation of cell-specific cytotoxicity enhancement by inhibition of mitochondrial ETC complexes i and III. *Photochem. Photobiol.* **88,** 1016–1022 (2012).

88. Rockwell, S. & Dobrucki, I. Hypoxia and radiation therapy: past history, ongoing research, and future promise. *Curr. Mol. Med.* **9,** 442–458 (2009).

89. Zannella, V. E. *et al.* Reprogramming metabolism with metformin improves tumor oxygenation and radiotherapy response. *Clin. Cancer Res.* **19,** 6741–6750 (2013).

90. Pore, N. *et al.* Nelfinavir down-regulates hypoxia-inducible factor 1?? and VEGF expression and increases tumor oxygenation: Implications for radiotherapy. *Cancer Res.* **66,** 9252–9259 (2006).

91. Kelly, C. J. *et al.* Regulation of O2 consumption by the PI3K and mTOR pathways contributes to tumor hypoxia. *Radiother. Oncol.* **111,** 72–80 (2014).

92. Siregar, J. E. *et al.* Direct evidence for the atovaquone action on the Plasmodium cytochrome bc1 complex. *Parasitol. Int.* **64,** 295–300 (2015).

93. Storozhuk, Y. *et al.* Metformin inhibits growth and enhances radiation response of non-small cell lung cancer (NSCLC) through ATM and AMPK. *Br. J. Cancer* **108,** 2021–32 (2013).

94. Fasih, A., Elbaz, H. A., Huttemann, M., Konski, A. A. & Zielske, S. P. Radiosensitization of pancreatic cancer cells by metformin through the AMPK pathway. *Radiat. Res.* **182,** 50–59 (2014).

95. Hurley, R. L. *et al.* The Ca2+/calmodulin-dependent protein kinase kinases are AMP-activated protein kinase kinases. *J. Biol. Chem.* **280,** 29060–29066 (2005).

96. Hawley, S. a. *et al.* Calmodulin-dependent protein kinase kinase-?? is an alternative upstream kinase for AMP-activated protein kinase. *Cell Metab.* **2,** 9–19 (2005).

97. Zhang, W. *et al.* Tamoxifen-induced Enhancement of Calcium Signaling in Glioma and MCF-7 Breast Cancer Cells Advances in Brief Breast Cancer Cells 1. 5395–5400 (2000).

98. Shackelford, D. B. *et al.* LKB1 inactivation dictates therapeutic response of non-small cell lung cancer to the metabolism drug phenformin. *Cancer Cell* **23,** 143–158 (2013).

99. Sullivan, L. B. *et al.* Supporting Aspartate Biosynthesis Is an Essential Function of Respiration in Proliferating Cells. *Cell* **162,** 552–63 (2015).

100. Ahn, C. S. & Metallo, C. M. Mitochondria as biosynthetic factories for cancer proliferation. *Cancer Metab.* **3,** 1 (2015).

101. Engelke, M., Bojarski, P., Bloß, R. & Diehl, H. Tamoxifen perturbs lipid bilayer order and permeability: Comparison of DSC, fluorescence anisotropy, Laurdan generalized polarization and carboxyfluorescein leakage studies. *Biophys. Chem.* **90,** 157–173 (2001).

102. Wiseman, H. Tamoxifen : new membrane-mediated mechanisms of action and therapeutic advances. *Trends Pharmacol. Sci.* **15,** 83–89 (1994).

103. Pelicano, H., Martin, D. S., Xu, R.-H. & Huang, P. Glycolysis inhibition for anticancer treatment. *Oncogene* **25,** 4633–4646 (2006).

104. Ran, F., Hsu, P., Wright, J. & Agarwala, V. Genome engineering using the CRISPR-Cas9 system. *Nat. Protoc.* **8,** 2281–308 (2013).

105. Kochanowski, N. *et al.* Intracellular nucleotide and nucleotide sugar contents of cultured CHO cells determined by a fast, sensitive, and high-resolution ion-pair RP-HPLC. *Anal. Biochem.* **348,** 243–51 (2006).

106. Basu, S. S. & Blair, I. a. SILEC: a protocol for generating and using isotopically labeled coenzyme A mass spectrometry standards. *Nat. Protoc.* **7,** 1–12 (2012).

107. Snyder, N. W., Basu, S. S., Zhou, Z., Worth, A. J. & Blair, I. a. Stable isotope dilution liquid chromatography/mass spectrometry analysis of cellular and tissue medium- and long-chain acyl-coenzyme A thioesters. *Rapid Commun. Mass Spectrom.* **28,** 1840–1848 (2014).

108. Aird, K. M. *et al.* ATM couples replication stress and metabolic reprogramming during cellular senescence. *Cell Rep.* **11,** 893–901 (2015).

109. Kridel, S. J. Orlistat Is a Novel Inhibitor of Fatty Acid Synthase with Antitumor Activity. *Cancer Res.* **64,** 2070–2075 (2004).

110. Jensen, M. M., Jørgensen, J. T., Binderup, T. & Kjaer, A. Tumor volume in subcutaneous mouse xenografts measured by microCT is more accurate and reproducible than determined by 18F-FDG-microPET or external caliper. *BMC Med. Imaging* **8,** 16 (2008).